

A Hydrodynamic Interpretation of the Tapeats Sandstone

Part II: Middle and Upper Tapeats

W.R. Barnhart*

Abstract

Bedforms and grain-size distributions in the middle and upper Tapeats Sandstone were analyzed to determine depositional conditions, including flow velocity, direction, and depth. I found that cut-and-fill structures were formed by high-density turbulent flow. Alternating compound cross-beds and high-velocity flat beds are the products of changes in depth and competency, possibly caused by cycles of one large storm wave followed by a secondary wave train. Foreset azimuth readings from cross beds indicate a large, unidirectional depositional current, moving northeast to southwest, and composed of many parallel tongues of deposition. Its vast extent and lateral consistency are seen in the ubiquity of tangential toe contacts on both large and small internal cross beds of the compound cross bedding throughout the formation. *Diplocraterium* ichnofossils in these tangential toe contacts shows an unexpected association of trace fossils with high-energy environments. Flow velocities were determined from grain size corrected to show the total preserved load, recognizing that deposited sediments represent mixed and bed loads *after* removal of much of the suspended load. Calculated velocities of over 4 m/s show that the entire Tapeats was rapidly deposited. A rhythmic pattern of bedforms supports that depositional rate. Conditions during Tapeats deposition are better understood by this hydrodynamic approach rather than through the use of facies models.

Introduction

As the bottommost member of the Cambrian Tonto Group in the Grand

Canyon, the Tapeats Sandstone has long been viewed as the first part of “a classic transgressive sequence of sandstone,

mudstone, and limestone that accumulated on the slowly subsiding Cordilleran miogeocline and adjacent craton” (Middleton and Elliot, 2003, p. 90). Deposited on the Great Unconformity overlying either Precambrian crystalline basement or tilted nonfossiliferous sedimentary sequences, the erosional

* W.R. Barnhart, c/o Creation Research Society, Chino Valley, AZ
Accepted for publication May 17, 2011

contact below the basal Tapeats is characterized by Rose (2006, p. 228, brackets added) as a “peneplain with only local relief in excess of a few meters per 100 m [328 ft] laterally.” The “local relief” typically refers to monadnocks found at eastern Grand Canyon and as far south as the Chino Valley in central Arizona (Figure 1, locations of monadnocks in Barnhart, 2012a, Figure 2). These Precambrian high are viewed as erosional remnants of the edges of tilted Precambrian sedimentary sequences. The classic studies of McKee (1945), Hereford (1977), and Rose (2006) all emphasized these features and interpreted the Tapeats as subtidal deposits sourced from the northeast. McKee (1945) saw evidence of reworking by tidal action in depths of less than 15.2–18.3 m (50–60 ft) of water. Hereford (1977, p. 209, brackets added) agreed that the sands were “deposited primarily on sandy intertidal flats...governed by the diminishing energy of tidal currents flowing shoreward across the gently-sloping tidal flats” under a flow depth of “between 5 and 10 m [16.4 and 32.8 ft].” Rose (2006, p. 234) viewed the Tapeats as a collection of “loose substrates of chemically inert sands and chemically reactive nonmarine paleosols” that moved and reacted “as tidal channels meandered and temporarily pooled and flowed, carrying and recombining various reactive clays, organics, and salts” in a unique pre-vegetated epicratonic estuary.

All of these authors saw the Tapeats as beach or nearshore sands (either above or below wave base) slowly developing on the flat peneplain broken occasionally by the eroded remnants of former marginal highlands. While aspects of their interpretations may be valid, careful analysis of the data does not always support them. The designation of the Great Unconformity as a “peneplain” and the varied composition of the monadnocks are a case in point. Neuendorf et al., (2005, p. 217) defined a peneplain as “a low nearly featureless, gently un-

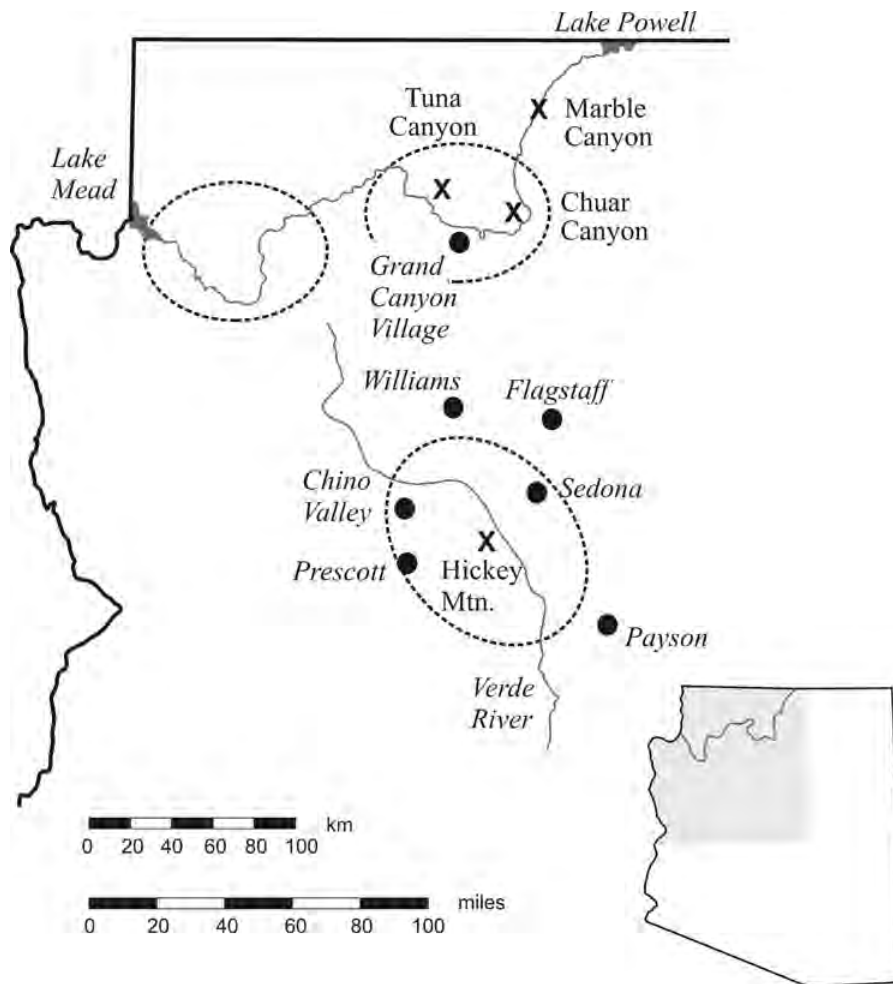


Figure 1. Location map of study area. X's mark locations discussed in text.

dulating land surface of considerable area.” Though the Great Unconformity is relatively flat, its apparent mechanism of origin does not fit the uniformitarian model. Oard (2011, p. 113, emphasis in original) contrasts plains and planation surfaces, with the latter observed to be eroded “independent of rock hardness on the regional scale.” Barnhart (2012a, 2012b) noted that the monadnocks are composed of rocks as soft as shale or as hard as quartzite, yet all are equally eroded and the highs are not restricted to the harder substrates. Therefore, the Great Unconformity is more likely an exhumed planation surface rather

than a peneplain. As Oard (2011, p. 117) observed, the continuous flatness of “planation surfaces are...formed... by some huge watery agency.” The relatively slow and selective erosional process envisioned by secular geologists cannot explain the broad, flat surface over such a large area. Furthermore, the monadnocks are not erosional remnants of marginal highlands, but remnants of a massive planation event, perhaps reflecting patterns of less energy in an otherwise highly erosive regional-scale current.

Barnhart (2012a) showed evidence that the lowermost Tapeats beds were

hyperconcentrated laminar bedforms deposited by high-velocity hyperconcentrated currents that were interrupted by cascades of loose breccia off the monadnocks that generated brief, high-density, turbulent flows depositing sandy debris flows. These events would have occurred simultaneously and during an event of higher energy and magnitude than any modern analog. The erosion and deposition under plastic flow conditions reflect elevated energy and preclude the common concept of low-energy processes on a passive continental margin. In short, the Tapeats is not a beach sandstone in the sense we understand it today.

This paper will look at bedforms in the middle and upper Tapeats. Those bedforms reflect a lower concentration of solids in the current and deposition under fluidal, not plastic, flow. If the Great Unconformity was eroded by high-energy, large-scale currents and the basal Tapeats was deposited plastically in high-velocity currents, then is it likely that the rest of the Tapeats reflects low-energy beach deposition on a slowly subsiding craton? It seems more likely that the rest of the Tapeats strata were also deposited in high-energy conditions. Bedforms and other sedimentary features in these beds will demonstrate that interpretation.

Hereford (1977, p. 199) described bedforms in the middle and upper Tapeats as:

large-scale cross bedding...that is characterized by compound cross-stratification, numerous reactivation surfaces, and herringbone pattern is typical of facies A and generally typical of finer-grained, thinner-bedded facies B. [These constitute] more than 95 percent of the bedding in the Tapeats Sandstone.

Rose (2006, p. 228) viewed these layers a little differently:

[They are] dominated by amalgamated channels of tangentially cross-bedded arkosic to subarkosic coarse to very coarse to gravelly sandstone. High-angle tangential cross-beds

(15°–60° foreset dips) can be traced along crude bedding planes a few to a few tens of meters into nested channels. Commonly only the gravelly bases of channels are preserved.

It is amazing that the quantity of work on these strata have yielded only generalized speculations about their origin. This emphasizes the fundamental failure of the facies model approach. In its place, I recommend an analysis of the hydrodynamic conditions of deposition that can be derived from sedimentary features such as bedforms and grains. That analysis will provide the basis for understanding the Tapeats in its entirety as a result of high-energy flooding across the planation surface of the Great Unconformity. These sedimentary features will now be examined in more detail.

Cut-and-Fill Bedforms

McKee (1945, pp. 126, 128, brackets added) described the bedding in the middle Tapeats.

Most of the modifications [from the common cross-lamination] are due to scour-and-fill development. Long narrow channels cut into normal [cross-laminated] beds and later filled with sediments dipping in and forward from both sides are characteristic of deposits near the flanks of monadnocks, although not confined to such localities. Scours that are similar in depth, but considerably wider and therefore proportionally shallower, are common at short distances from the monadnocks and near their bases, beyond the areas affected by initial dip.... The narrow channel-fill deposits... may possibly have formed by rip currents.

While McKee (1945) fails to distinguish here between “scour-and-fill,” “channel-fill” and the “debris-flow deposits” of Barnhart (2012a), he is definitely describing what I will call “cut-and-fill deposits.” He associated these cut-and-fill deposits with monadnocks and their

associated debris-flow deposits, although the cut-and-fill deposits are not unique to the monadnocks.

Hereford (1977, p. 205, brackets added) described his facies D (in central Arizona) as:

a coarse-grained sandstone to granule conglomerate characterized by small-scale trough cross-stratification filling erosional scours and numerous thin lenticular sandy shale and coarse siltstone partings. ... Thin layers of granule conglomerate line the base of many of the erosional scours. The tops of the sandstone beds are densely covered with *Corophioides* [an ichnofossil] burrows...reversals in foreset azimuths are common.

He agreed with McKee that the “small-scale trough cross-stratification” were cut-and-fill deposits. However, the evidence suggests that they instead are the products of debris flows (Barnhart, 2011).

Rose (2006, p. 228) described bedding in the middle Tapeats.

High-angle tangential cross-beds (15°–60° foreset dips) can be traced along crude bedding planes a few to a few tens of meters into nested channels. Commonly only the gravelly bases of channels are preserved.

In contrast, I identify the “nested channels” and “gravelly bases of channels” as cut-and-fill deposits (Figure 2).

While McKee (1945) took a practical view towards the cut-and-fill structures in light of his interpretive model, attributing them to “rip currents,” it is important to understand that channels are cut by *any* high-energy current not in balance.

Any current carrying sediment is constantly in an energy balance. The work scale is a continuum from high-energy erosion and a sediment load at one end, through sediment transport in the middle equilibrium range, to lower energy conditions with sediment deposition. Most currents shift between these ranges. If the slope is steep, the

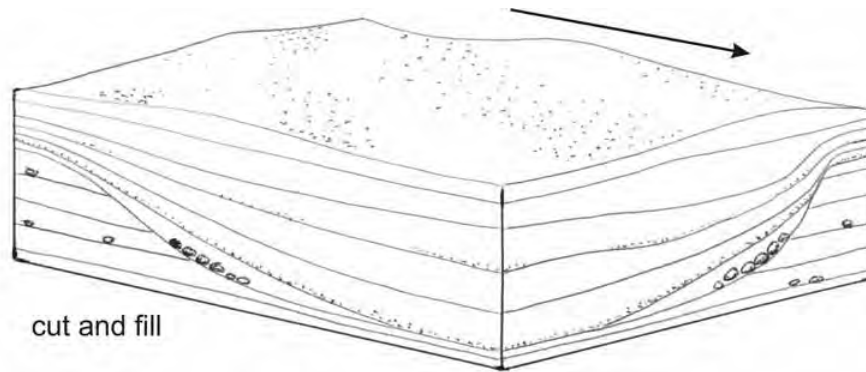


Figure 2. Cut-and-fill block diagram.

sediment load is small, and the substrate is unconsolidated, the current will erode into the substrate to create a flatter slope, trying to reach an equilibrium between energy and sediment load. But if the sediment load is too great, it will exceed carrying capacity and initiate deposition (Schumm and Khan, 1972). The resulting bedform will be a product of the sediment load affected by the rhythmical flexing of drag and release exerted by the buildup and release of shear stress in the boundary layer (Barnhart, 2012a). This makes the bedform a function of flow velocity, not available energy, although unique energy fluctuations may be expressed in unique variations, such as seen in the compound cross beds of the Tapeats.

The traction layer, occurring as the bottommost layer of a debris flow (Barnhart, 2011, figures 5 and 6), is composed of a fine sand fraction but only forms in a debris flow above an unconsolidated substrate. The sequence of bedforms in a debris flow can be confusing. As the basal layer, the traction layer must form first in a high-density turbulent flow. Since fine sand is the fraction most likely to be in suspension, a traction layer of fine sand could be unexpected. But the resuspension of the fine sand fraction from the substrate layer occurs as the highly turbulent head of the flow forces water down into the viscous sublayer.

Not only is this a good example of the significant interaction between the head of a high-density turbidity flow, but it is also a strong indication of extra energy being expended. If there is enough excess energy in the head, a debris flow can erode flute marks into the substrate as deep as 2.4–3.0 m (8–10 ft) (Sohn et al, 2002, their figure 6C).

There is a fine balance between energy and sediment. Too little sediment allows turbulency vectors to erode the substrate. Too much sediment results in deposition, as the current cannot maintain it in suspension. In that continuum, at a slightly higher energy level than needed to produce a traction layer, but less than needed to cause flute erosion, the current is strong enough at its head to create the “cut” of a cut-and-fill sequence, while the flat beds of the fill are produced by the lower energy level of the body and tail of the current. These are not low-energy features; the fill includes both high-velocity flat beds and even horizontal compound cross bedding. There are no internal collapsed bedforms expected in low-velocity flat beds. Laminae show separation by a developed parting lineation, indicating deposition from a current carrying lower concentration of solids than the hyperconcentrated laminar flow that deposited the basal Tapeats (Barnhart, 2012a, figure 13).

If these cut-and-fill channels formed by tidal rip currents (McKee, 1945) or sandbar drainage channels (Klein, 1970), then they should show a series of tangential adjustments along their edges, reflecting repetitive flow back and forth through the same channel, such as repeated cycles of ebb and flood tides. Klein (1970, p. 1098) describes such channels formed on sandbars and mudflats of Minas Basin, Bay of Fundy, Nova Scotia as “semipermanent meandering and straight channels” which serve to drain not only tidal currents but also facilitate the “dewatering of the [surrounding] bar sediments.” This ongoing pattern leaves its marks in small patterns of tapered wedge-shaped deposits along multiple edges. Even if the cut channel had not gone through multiple tidal cycles, the dewatering of surrounding sediment alone would have blurred and deformed the edges of the cut.

By contrast, cut-and-fill features in the Tapeats were shown by McKee (1945, p. 44, his figure 5g) as a clean cut into cross bedding, followed by thin, flat laminae that reflect the flatness of the water surface, not the irregular shape of the bottom. The flat beds typically match the internal bedforms of the cross bedding (Hereford, 1977, p. 208, his figure 9). These bedforms, as shown in the next section, can be produced *only* under high-velocity flow. The lack of reworking along the edges requires deposition of a continuous influx of sediment, strongly suggesting a continuous unidirectional current (Barnhart, 2011, 2012a).

The ubiquitous repetition of relatively narrow channels suggests an incredibly broad current that split along its leading edge into localized tongues of increased turbulence. The following current must have been relatively shallow to produce the thin flat beds filling the channels. The restriction of the first layers to the cut channels show that the cut-and-fill was deposited by one event. The narrow tongues are seen to be part

of a much larger current because at the tops of the channels, the bedding spreads out laterally without interruption, without eroding the channel edge into a rounded form.

Compound Cross Bedding

Flat beds are ubiquitous in the rock record. Flume and field data have verified that simple flat beds form in three instances of fluidal rheology: (1) low-velocity flat beds, (2) antidunes, and (3) high-velocity flat beds. Barnhart (2011, 2012a) determined that they can also be the result of various plastic flows, but the middle and upper Tapeats beds were not deposited under plastic rheology.

Low-velocity flat beds occur when low-velocity ripples form in coarse sand and the ripples collapse due to the large grain size. Antidunes are a high-velocity bedform, forming flat beds when the surface inline waves collapse, sending shock waves through the vertical fluid column that collapse the antidune bedforms. Flat beds produced by the collapse of low-velocity ripples and high-velocity antidunes both show the distorted internal lamination (Barwis and Hayes, 1985, p. 910, their figure 7).

The formation of high-velocity flat beds was investigated at Colorado State University, Fort Collins, Colorado in a 0.15 m x 0.15 m x 2.4 m (0.49 x 0.49 x 7.9 ft) flume (Julien et al., 1994). Figure 3 demonstrates how an apparent flat bed is built up from a prograding slope front. The length of the cross beds is determined by the thickness of the flat beds. Internal cross beds develop until a positive slope of the flume increases “up to the limit of the angle of repose (30° to 40° for sands), the lamination [top surface] of sediment is parallel to the slope” (Berthault, 2002, p. 445, brackets added). These tilted flat beds would likely be classified in the field as cross beds, and if internal depositional cross bedding can be discerned, the resulting bedform is called *compound cross bedding*.

Barnhart (2011) noted that the association of cross bedding with recurring flat beds indicates a change in competency, not flow velocity. Competency is the ratio of flow velocity and flow depth resulting from a sudden increase in flow volume. If flat and cross beds are produced by identical rheological conditions and an increase in flow depth that allows the layer to grow thicker as compound cross bedding, then both

cross bedding and flat beds should be considered as occurring under similar conditions. Compound cross beds (Figure 4) are high-velocity flat beds deposited on an incline and showing internal cross bedding formed during deposition. When sloping compound cross bedding is interbedded with horizontal flat beds, both were likely deposited under the same conditions except for intermittent changes in competency.

Additionally, because the internal cross bedding is a high-velocity bedform, any interruption of the flow would result in the formation of smaller, superimposed, low-velocity ripples or the washed-out, low-velocity flat beds they produce as velocity drops. In their study of bedforms in San Francisco Bay, California, Rubin and McCulloch (1980, p. 224, 225, brackets added) point out:

Small bedforms [low or high velocity] superimposed on larger ones are not merely a curiosity. They appear to be the rule rather than the exception.... Large bedforms generate boundary layers in which smaller bedforms can exist.... At shear velocities that are higher in the sand-wave range, upper flat beds formed at sand-wave crests and ripples [low velocity] were restricted to lower shear-velocity flow in the troughs.

Smaller superimposed bedforms will develop at the boundary layer of larger bedforms with velocity change; either lower or upper flow regime superimposed bedforms will develop if any depositional parameters are changed. The absence of superimposed low-velocity bedforms or their remnants suggests that each of the thick compound cross beds was deposited by a single uninterrupted unidirectional current (Barnhart, 2011). Since the compound cross beds and the horizontal flat beds above and below are genetically related, the absence of small, superimposed low-velocity bedforms indicates that the horizontal beds were deposited sequentially with the diagonal

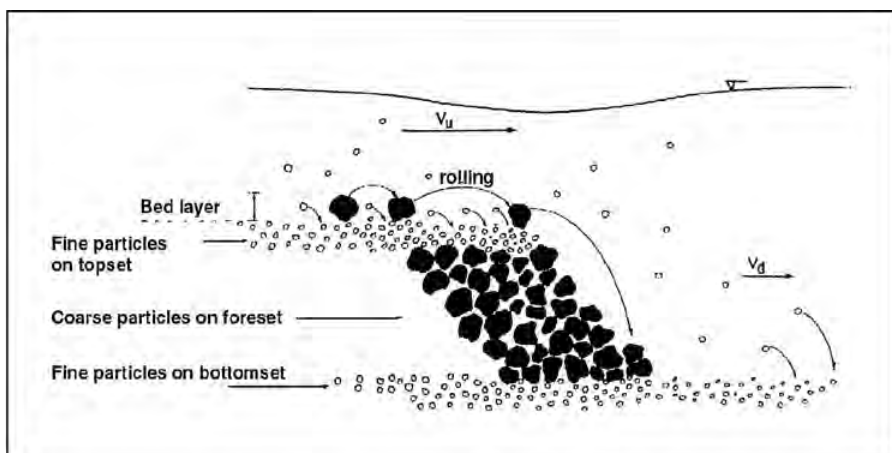


Figure 3. Sequence of deposition in high-velocity flat beds as determined by flume experiments (Berthault, 2002, his figure 3). Cross bedding may not be visible but is obviously present.

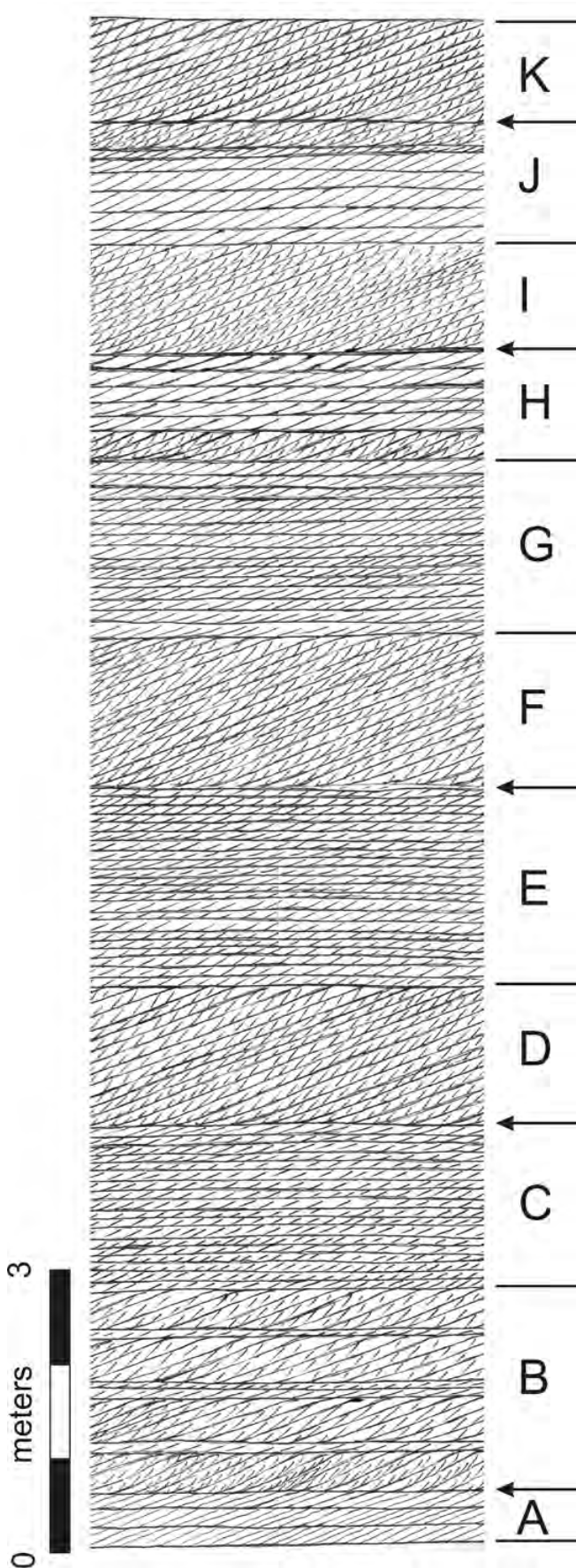


Figure 4. Compound cross bedding of middle Tapeats in Marble Canyon, eastern Grand Canyon at Colorado River. Repetition sequences begin at arrows; see text for discussion.

layers in a continuous unidirectional current.

In the Tapeats, compound cross bedding is seen at Marble Canyon (Figure 4), in the eastern end of Grand Canyon (Figure 1). In the middle to upper Tapeats, strata are deposited in both distinct forms. Horizontal flat beds are seen in layers C, E, H, and J of Figure 4, and cross beds in layers D, F, and I. The angle of the layers in D and F as measured from a photograph are 24° – 26° , and the angle of the smaller compound cross beds are also 24° – 26° , as measured at multiple locations in the photo. The two measures combine to give an angle of 48° – 52° for the smallest cross beds—an angle much greater than any expected angle of repose. All parting surfaces give an appearance of tangential toe contacts (Nichols, 1999, p. 48) on every cross bed, as confirmed by Rose (2006).

Hereford (1977, p. 201) documents similar compound cross bedding (his figures 3 and 4) in the Chino Valley area (Figure 1). He states:

Beds with compound cross-stratification are the thickest found in the Tapeats; thicknesses between 1 and 3 m are not uncommon, with the foresets as thick as 10 cm.

He identifies the angle of dip as 24° on the sloping flat beds; the smaller cross bedding in his photograph exhibits dips of 24° – 26° .

Both the Marble Canyon and the Chino Valley outcrops of the middle Tapeats align with the axis of deposition, northeast to southwest, and it “constitutes more than 95 percent of the bedding in the Tapeats Sandstone” (Hereford, 1977, p. 199). This suggests that the Tapeats was a continuous depositional body, remarkably similar across more than 200 km (124 miles). This sand body was over 300 km (186 miles) wide and 120 m (393.7) thick at the Bass Trail (Middleton and Elliott, 2003). Obviously this would require consistent depositional conditions over

a large area; in the case of the Tapeats, a large unidirectional current.

The photograph from which Figure 4 is taken shows a 0.5 to 1 km (0.3–0.6 mile) stretch of the Tapeats in Marble Canyon. Major stratal features are clearly visible and continue uninterrupted. By contrast, in Chino Valley, Hereford (1977, p. 201) noted that “thick sets of cross-stratification are commonly cut diagonally ... by two or as many as ten planar or curved surfaces” (Figure 5.1). These terminal edges may be unique to the central Arizona region and may well indicate the termination of the depositional tongues of the larger current. Hereford (1977) identified these curved diagonal surfaces as *reactivation surfaces*, where erosion beveled the edges of the original deposit. Similar features were noted on a smaller scale around the depositional perimeter of splay deposits formed during the levee breaches during Hurricane Katrina (Barnhart, 2011). Though found around all edges of the deposit, they are not erosional surfaces formed in a later event.

Nelson and Leclair (2006) identified the distal edges of the splay as < 0.3 m (0.98 ft). They did not taper to zero in a tangential manner, as would be expected from erosion. This is consistent with the edges in Figure 5.1. As Barnhart (2011) determined, the entire thickness and extent of the deposit, including the nature of the distal edges, was formed by a single continuous unidirectional current. Therefore, the three bedding divisions shown in Figure 5.1 are the terminal ends of sediment deposited by three individual waves with no intervening erosional events. Furthermore, the absence of smaller superimposed bedforms suggests that the three episodes of deposition were nearly simultaneous; probably they represent tongues of deposition from the same overall current.

The terminus of deposition definitely is not the same geographically as the extent of the current. The Katrina splay deposits had a distal edge of only about

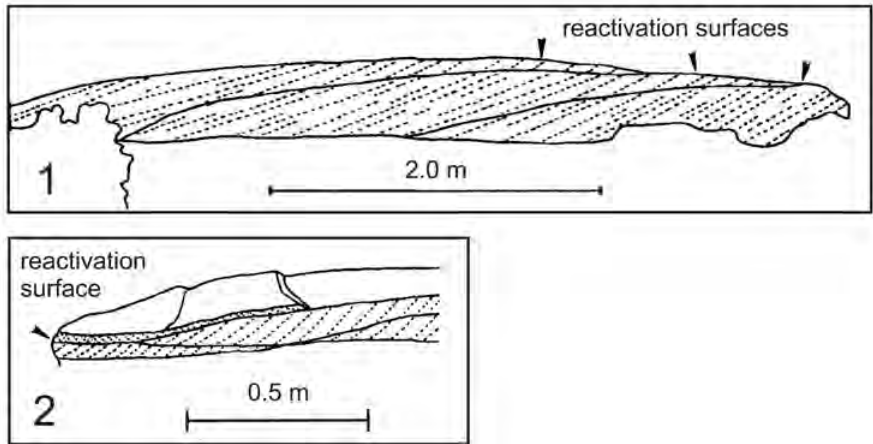


Figure 5. Occurrences of compound cross bedding in central Arizona near South Butte, showing orientation of internal cross bedding. 5.1: Reactivation surfaces are uneroded edges of lobate flow. 5.2: Occurrence of reverse cross bedding produced by antidunes. Modified from Hereford (1977, his figures 3A and 3B).

400 m (1,312 ft) from the canal breach, but the water flowed an additional 6–10 km (3.7–6.2 miles) to fill the entire basin of New Orleans to the level of Lake Pontchartrain. It is crucial to note that sediment thickness and extent were not controlled by the extent of the flow but by its *competency*. The two most significant factors for competency are (1) solids concentration and (2) flow depth. The distal edges of the Hurricane Katrina splay formed under a very rapid flow of up to 2.73 m/s at relatively high solids concentration of 20%–30% (Barnhart, 2011).

Herringbone Pattern of Reverse Cross Bedding

Herringbone pattern cross bedding (Figure 5.2) was found by Hereford (1977, p. 201, 203) in central Arizona, where he noted in his facies A and B “fairly common occurrence of herringbone pattern.” He attributes those bedforms to intertidal sandbars based on Klein’s (1970) study, or transverse bars in braided streams studied by Smith (1972).

Klein (1970) did find herringbone patterns in tidal environments, specifically in Minas Basin, Bay of Fundy,

Nova Scotia. There he documented it in several compound bedforms (Figures 6 and 7). In these figures, the layer of reverse cross bedding measures about 30 cm (0.98 ft) and 10–20 cm (0.32–0.66 ft) respectively. The illustrations show alteration of flood and ebb tidal currents over multiple cycles and two cycles, respectively. Figure 7.1 shows that reworked sand is predominantly oriented by the flood (incoming) tide, and Klein (1970) attributes the reverse cross bedding lower in the section to stronger currents during spring tides. In Figure 7.2, where reversed cross bedding was formed by one day’s normal tidal reworking, the thickness of ebb tide reverse cross beds is the same as that of the flood tidal deposits, except for dune surfaces that were not reworked.

Transverse bar deposits consist of two distinct types of layers (Figure 8), the larger cross-bedded layer (B) that forms at the leading edge of the migrating bar, and the small low- and high-velocity bedforms (A, C) deposited by the shallow, slower flow prior to the bar’s arrival and then by the boundary layer of the elevated surface of the larger cross beds. It is the migration of these small, superimposed bedforms (C) as they “walk

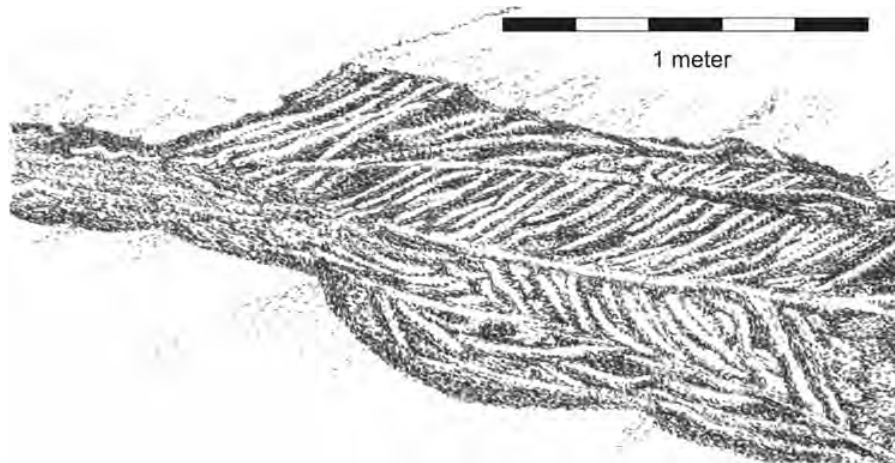


Figure 6. Bidirectional deposit between second and third layers separated by thin layer of decreased flow small bedforms (mostly low-velocity plane beds) in sand bar or sand wave. Trenched cross section with real reactivation surfaces. Ebb current to left, flood current to right. West Bar, Minas Basin, Bay of Fundy, Nova Scotia, Canada (Klein, 1970, p. 1116, his figure 27D).

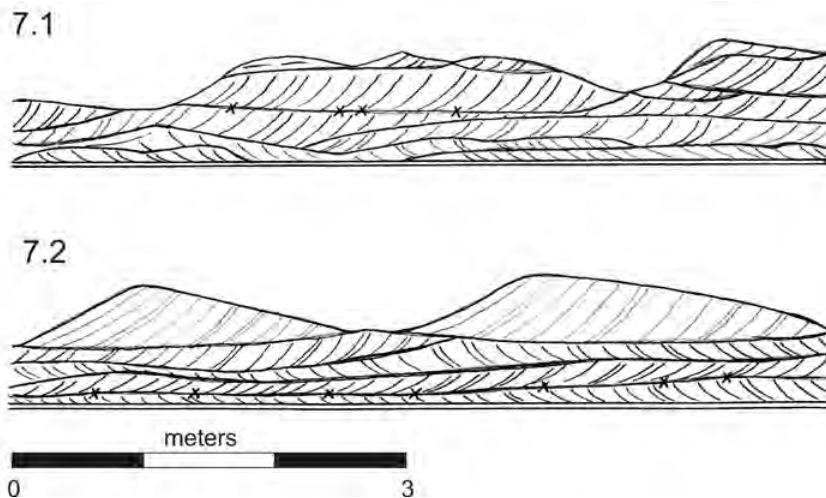


Figure 7. Herringbone cross bedding, evidence of bidirectional flow under tidal conditions. Sandbar at Economy Point, Minas Basin, Bay of Fundy. 7.1: Midtide reworking, August 1, 1968. 7.2: Maximum tide reworking, August 9, 1968. The "x" marks depth of reworking after two tidal cycles (24 hrs.) during maximum spring tides. Modified from Klein (1970, his figures 32A and 32B).

off" the front edge of the bar (Figure 9) that provides the primary source of sediment for the migrating bar. Smith (1972) described reverse cross bedding in both layers of the transverse bars of the

Platte River, Nebraska. He interpreted the larger ones as forming near the bar margin, where merging currents and eddies reversed the orientation of the bar margin, swinging it almost completely

contrary to downstream flow. He interpreted the small reverse cross bedding as secondary, small-scale antidunes that formed superimposed on top of the bar when the ratio of flow velocity to depth on top of the bar was higher due to a decrease in depth. Smith's (1972) reverse azimuth readings constituted about 2–5% of total measurements.

Barwis and Hayes (1985) also documented the formation of small antidunes of 0.5–2.0 cm (0.2–0.8 in) atop a wash-over fan on top of a seaward berm bordering Seabrook Island, South Carolina. The berm crest, about 1.54 m (5 ft) above mean sea level, acted as a weir for breaking waves, causing them to experience a hydraulic jump to supercritical flow as they overtopped the berm. While Smith (1972) did not give a hydrodynamic explanation for the origin of the small-scale antidunes he observed, the genesis would likely be very similar—a continuous unidirectional current running across either berm or bar at increased velocity as the depth decreased. Neither example conforms to Klein's (1970) example of tidal deposition. Thus, these bedforms can be deposited in environments other than tidal.

Two distinct varieties of reverse cross bedding in the Tapeats were documented by Hereford (1977). In Figure 10, the reverse cross beds are of nearly equal height as the normal cross beds above and below (Layers 9, 13, 16, and 18). These are likely not tidal facies, since all are genetically related; they were deposited at approximately the same time. That interpretation relies on the absence of reworking or separate walking dune structures as shown by Klein (Figure 8).

Figure 6 shows three layers in a trench on a sandbar, including those of reversed azimuth. Note the three layers are of roughly equal height, each separated by a distinct layer of smaller bedforms. These flat laminae did not form by the simple settling of the fine fractions (Figure 3) because they pos-

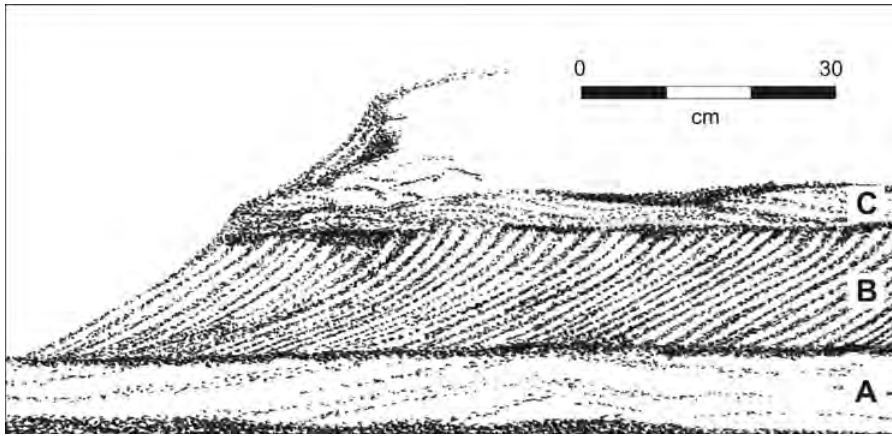


Figure 8. Trenched cross section of transverse bar from Platte River, Nebraska, showing alternating layers of (A) low-velocity flat beds underlayment, (B) alternating cross-bedding of fine and coarse grains, and (C) bed of small low-velocity bedforms left on top surface. Modified from Smith (1972, his figure 3).

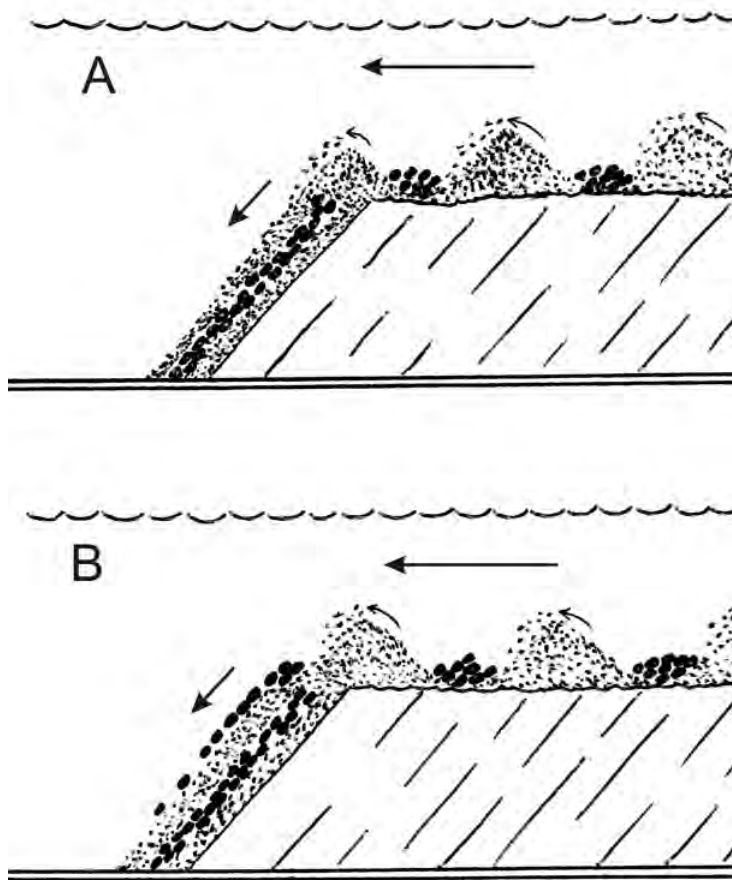


Figure 9. Laminae of cross bedding in Figure 8 showing method of deposition by cascading small low-velocity bedforms walking down current to bar surface. Modified from Smith (1972, his figure 4).

sess the distinct wavy appearance of washed-out ripples and are probably low-velocity flat beds. This is the transition that would be expected as current velocity slows to turn direction of the prominent flow from ebb to flood and back to ebb tides.

In the middle Tapeats, the cross bedding is obvious (Figure 10), but nowhere in the Tapeats has this author seen the stoss slope of a dune. Some should exist, but if the depositional environment was similar to that of the Katrina splay deposits, they would be rare because elevated flow velocity would produce longer wave length, and thus fewer dunes and fewer stoss slopes. Instead, dunes would appear as rapidly progressing transverse bars, prograding not by the migration of small bedforms across their surface, but by direct sedimentation of sloping flat beds down the lee slope. The deposit's height would then be limited only by the depth, with no time to generate small, superimposed bedforms on top.

Another possibility is that higher concentrations of solids would result in no stoss slopes (Barnhart, 2011, 2012a; McKee et al., 1967). Again, the sloping, prograding flat beds would continuously keep the bedform moving with the current as a transverse bar. Figure 10 in layers 13–27 shows overlapping tongues of sediment, each with limited lateral spread but showing evidence of the edges interacting with different current vectors, such as eddies, as documented by Smith (1972).

The second variety of Hereford's (1977) herringbone pattern bedding is shown in Figure 7.2, where the thin laminae of reverse cross bedding, about 2 cm (0.78 in) thick, overlie a bed 4–10 cm (1.6–3.9 in) of normal cross bedding. These proportions suggest that antidunes formed secondary bedforms superimposed on a ridge of previously deposited sediments, as documented by Smith (1972) and Barwis and Hayes (1985).

Both occurrences of reverse cross bedding in the middle Tapeats can

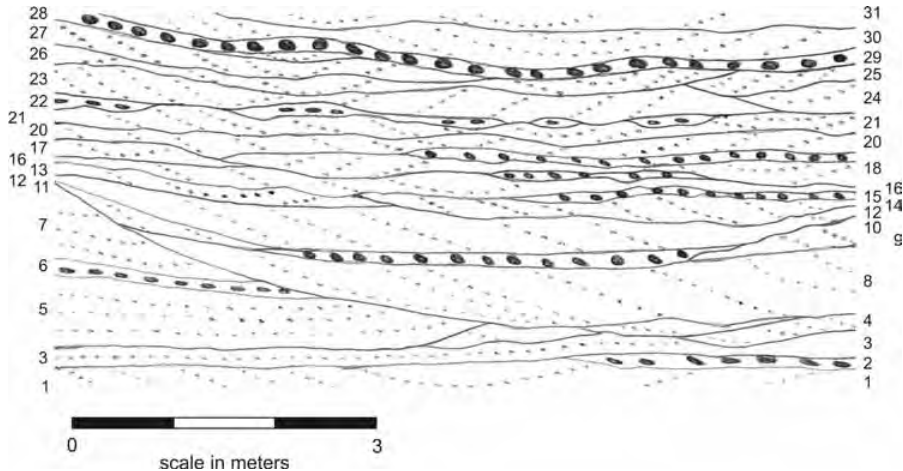


Figure 10. Vertical exposure of middle Tapeats north of East Verde River showing diverse orientations of foresets within individual numbered layers at a single location. Modified from Hereford (1977, his figure 9; note Hereford's image was upside down).



Figure 11. Ichnofossil traces in tangential toe contact of upper Tapeats at Tuna Canyon (Rose, 2006, his figure 3C). Note boundary at top and bottom of ichnofossils created by differences in cementation. Bar is about 5 cm. Top is presumed to be a bedding surface of foreset about 10 cm thick, based on thickness of next layer between arrows.

be better explained by deposition, as tongues of sediment persisted in a unidirectional current, rather than as tidal deposits. With little indication of reworking beyond the cut-and-fill structures, it is evident that the flow carried sufficient solids for continuous deposition along the advancing current's front and also in pulses representing wavelength intervals superimposed on that current.

Tangential Toe Contacts and Ichnofossils

Rose (2006, p. 228) describes tangential toe contacts in the middle and upper Tapeats, calling them "tangentially cross-bedded arkosic" layers, adding,

U-shaped burrows (*Arenicolites*) are sparsely present in planar horizons throughout much of the Tapeats Sandstone but are common in the upper parts of typical Tapeats sections, where they occur on steep tangential foresets.... Tangential foresets are not obviously bundled wherever they occur ... nor do they occur en echelon ... and therefore do not contribute to the interpretation of tidal origin.

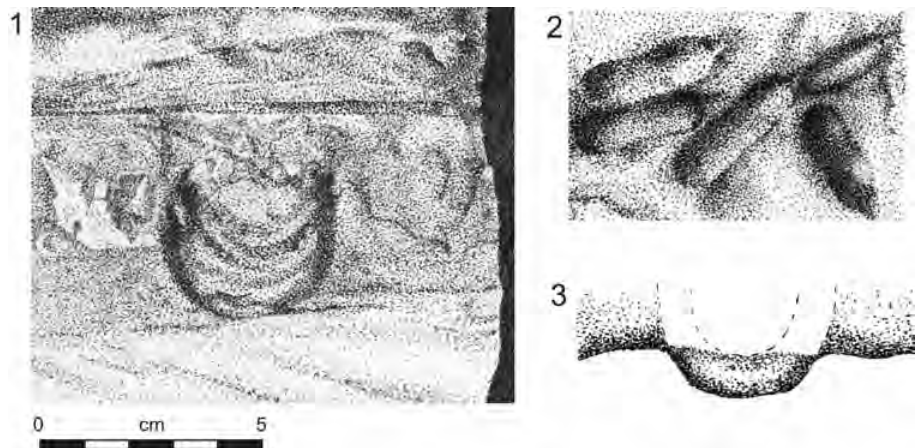


Figure 12.1. Ichnofossil traces of *Diplocraterium* showing spreite within U-shape and upper and lower boundaries of differential cementation. 12.2. Traces of *Diplocraterium* showing torpedo shape of lower bend of tube as it projects on many under surfaces (Hereford, 1977, his figures 8A and 8B). 12.3. Side view of traces.

This is in line with Barnhart (2011), who showed that Katrina splay deposits exhibited tangential toes on cross bedding as a result of high-velocity flow. These contacts manifest the strength and velocity of the vortex that prevents cascading of gains down the lee slope of the dune. Therefore, the stronger the vortex, the more pronounced the

tangential contacts, and the faster the current.

Thus, ichnofossils in a tangential toe contact require deposition under high-velocity conditions, not the low-energy environment of lengthy bioturbation on top of the sand. Both of these are conditions generally not expected for ichnofossils (Coward and Froede, 1994)

and represent even more rapid intrusions of substrate than the fastest rates determined for modern marine filter feeders (Froede, 2009). The burrows are labeled *Arenicolites* by Rose (2006) and *Corophioides* by Hereford (1977). Figure 11 is from Rose (2006) and shows well-developed burrows on a tangential toe contact in Tuna Canyon (Figure 1). Although the photo's size and weathered surface on the fossil do not allow for visualization of spreite on the interior of the U-shaped burrows, it does clearly show their occurrence within the tangential portion of the deposit. Spreite were clearly visible on all U-shaped burrows observed by the author in the upper Tapeats and are well illustrated in the *Corophioides* shown by Hereford (1977) in Figure 12, near Hickey Mountain. Mason and Christie (1986, p. 249) showed that *Corophioides* "are assigned to ichnogenus *Diplocraterium*" and will be referred to as *Diplocraterium* subsequently in this paper.

Mason and Christie (1986) equated the presence of *Diplocraterium* with marine deposition, positing a marine basin in the northeastern Karoo Supergroup in South Africa, primarily because of the local presence of the ichnofossils. Likewise, Hereford (1977) equates *Diplocraterium* (*Corophioides*) with marine conditions. Sandstone beds where *Diplocraterium* occur in very dense colonies are never more than one burrow deep in a single depositional layer, and none are obscured by bioturbation. Therefore they likely developed simultaneously in a short period of time. Hereford (1977) attributed these deposits to a tidal channel.

Figures 12.2 and 12.3 show the base of the lowest curve of the burrows, commonly seen on partings of overturned rocks. Large clasts containing these features are scattered along the edge of the Tonto Platform in the upper Tapeats. Curiously, the rocks' cement often changes abruptly at both the upper and lower surface of the *Diplocraterium* burrow. Although little or no evidence of

organic residue is found in the burrows, the change in cement composition may indicate the influence of the decomposing organic remains of the trace makers.

The presence of spreite within the U of the burrow (Figure 12.1) is thought to indicate that the organism burrowed down into the substrate by distending first one part and then another of a segmented body. The burrows always appear on the surface of the substrate as a small groove terminating at each end in a hole and are sometimes called "staple marks." But no rubble from the hole was moved up to the surface, nor is any lifting of the substrate visible around the holes. This is unusual since burrowing filter feeders invariably leave a pile of substrate sediment beside or around their burrows (Froede, 2009, his figure 1). Thus, the burrow was excavated into the sand prior to compression and compaction when the sand's surface was formed, suggesting that the organism had to arrive in the same current with the sand. If the sand was transported at a high current velocity, then the same is true of the organisms responsible for the *Diplocraterium* burrows.

Diplocraterium on tangential toe contacts shows that the organisms arrived in great numbers in high-velocity currents. Their demise would have altered the chemistry of pore fluids, which resulted in rapid cementation. Thus, *Diplocraterium* appear to be escape burrows, not feeding structures. Other ichnofossils are thought to be a result of travel or feeding trails. Since most of these are very short in length, a few cm to a few tens of cm, they may have been formed between pulses of deposition. Their increasing abundance in the upper Tapeats may indicate an increased interval between waves as sand deposition waned and ceased. Longer "foraging" ichnofossils may have formed shortly after deposition but before compaction and cementation. Many of these "feeding" or "foraging" trails may actually represent escape structures by

the organisms and the conditions under which they had to function.

Paleocurrents and Cross-Bedding Azimuths

Hereford (1977) measured 727 azimuth readings of cross-bed foreset inclinations at 13 locations in the middle and upper Tapeats in central Arizona. Given the large area, the number and distribution of these measurements, these should be seen as a random sample. However there are several interesting trends that can be seen in these measurements. His rose diagrams (Figure 13) with arrows show the general deviation and vector-averaged direction for each location. He divided these locations into three groups (Group I = 1–4, Group II = 5–8, and Group III = 9–13), and these groups show a decrease in azimuth variation toward the east. Hereford (1977, p. 203) noted: "Groups I and II could be expected to develop on intertidal sandbars by deflection of tidal currents around irregularities on the depositional surface (Klein, 1970) ... [and] are similar to distribution shown. ... from a modern braided river."

But Schumm and Khan (1972, p. 1755) determined that "streams or currents will only braid on slopes > 0.016." Calculations (Barnhart, 2012a) show that water flowing down that great a slope would have been too shallow to deposit the thickness of layers seen in the basal Tapeats. Needless to say, this would be even more improbable in the thicker strata of the middle and upper Tapeats.

Klein (1970, p. 1109) showed foreset inclinations of diverse azimuth do occur on intertidal sandbars: "The conclusion is therefore inescapable that this elliptical pattern of sand transport though both flood- and ebb-dominated portions of tidal sand bar is a characteristic transport pattern for intertidal and subtidal sand bodies." His figure 18 shows rose diagrams roughly symmetrical over 60°–180° spreads with the greatest number of readings in the central range.

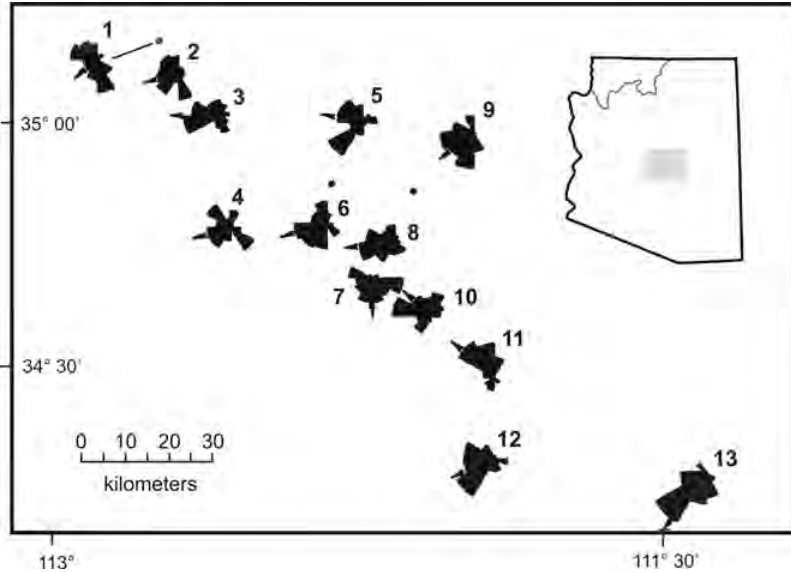


Figure 13. Rose diagram from Central Arizona measured by Hereford (1977, his figure 6) showing direction by percentage of azimuth reading from foresets for each location.

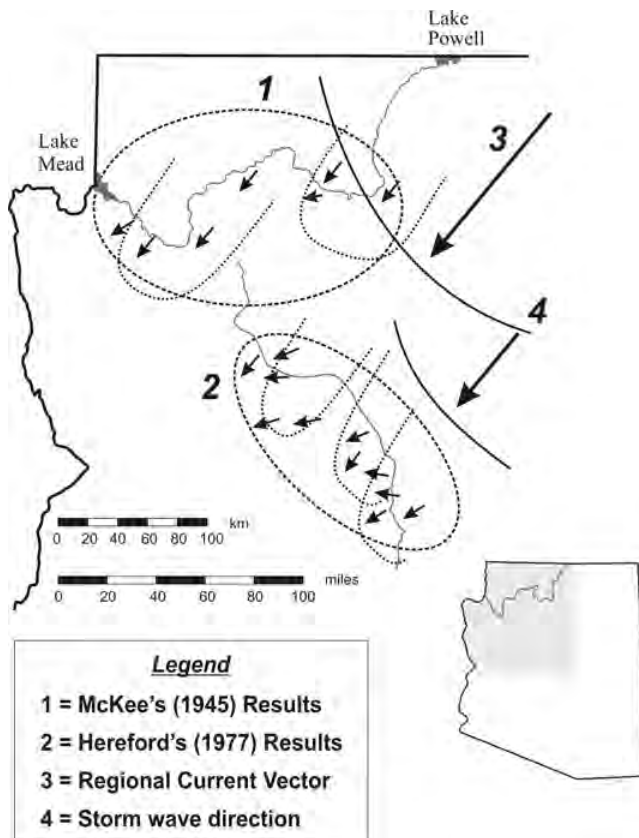


Figure 14. Pattern of lobate deposition in middle and upper Tapeats suggested by distribution of foreset inclinations. Data from McKee (1945) and Hereford (1977).

Smith showed similar diverse foreset inclinations in transverse bar margins in braided streams form as a lobate arrangement. His figure 11, while showing a pronounced preference for the direction of fluvial flow, also shows a logarithmic distribution for 80° on either side of the current. Specifically he recognized “only 40.5% of the foresets measured are oriented within 5° of the current which formed them ... and 86.1% within 45°” (Smith, 1972, p. 630).

A comparison of McKee’s (1945) paleocurrent measurements with Hereford’s (1977) rose diagrams shows that no groups fit the patterns described by Klein (1970) or Smith (1972). Instead, they form one-half of an ellipse covering the entire > 300 km (> 186 miles) across the map (Figure 14). McKee’s (1945) and Hereford’s (1977) Group I form the side of the very wide tongue, while his Group II would be west of the center blending into Group III, the primary current vector.

Hereford (1977, p. 203) suggested “deflections ... around irregularities of the depositional surface” as a reason for his azimuth variations. However, the only significant irregularities on the surface of the Great Unconformity were low monadnocks, and those are restricted to the eastern part of the study area (Barnhart, 2012a, figure 2). In fact, Figures 13 and 14 show the monadnocks occurring precisely where azimuth readings become more regular with less deflection, exactly the opposite of Hereford’s (1977) prediction. In the central and western part of the study area—defined by Rose (2006) as a level penplain without significant vertical variation—current deflections should be less common. McKee (1945, pp. 128–129) said of the monadnocks in the Bright Angel quadrangle,

Only slight variation from the regional direction of movement is indicated even in those sediments that are close to the ancient land

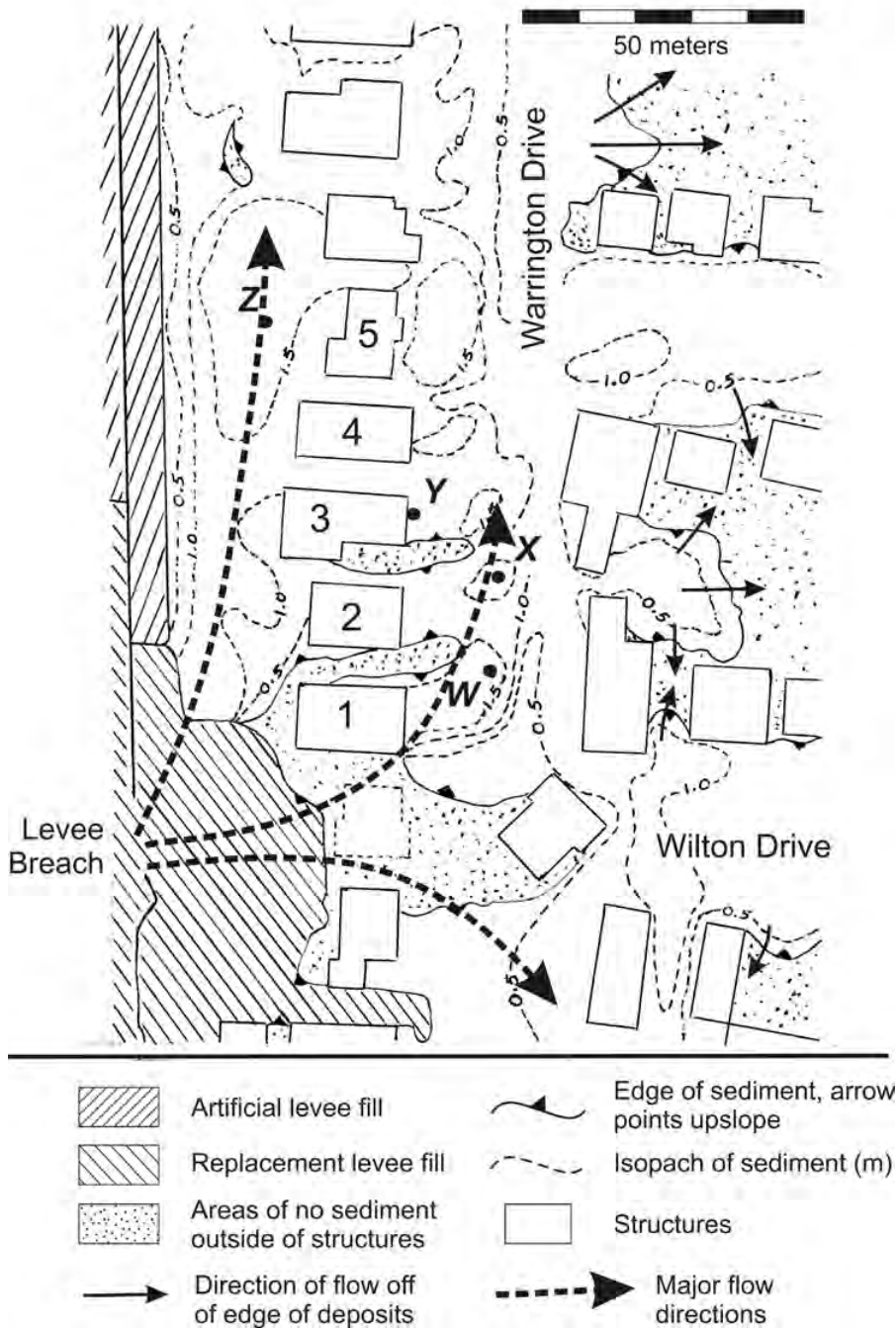


Figure 15. Hurricane Katrina deposits in New Orleans from a single breach in the London Avenue Canal. Dashed lines show major direction of flow around obstructions. Solid arrows show diverse azimuth readings of foreset inclination around tongues at perimeter. From Barnhart (2011).

masses. The conclusion is reached, therefore, that these hills had little influence on the actual deposition near their sides.... Beds of the Cam-

brian sandstone slope away from the hills in all directions, largely as a result of post-consolidations compaction over a hard center ... yet, the

cross-lamination within these beds are constant in direction.

So Hereford's (1977) explanation of deflection around obstacles does not explain variations in direction of flow in the Tapeats Sandstone. Paleocurrent measurements are better explained by seeing the depositional medium of the Tapeats as a broad current of great energy (Figure 14). The levee breaches during Hurricane Katrina demonstrated that azimuth readings will radiate out from the point of origin of the flow, in that case the levee breach (Figure 15). It follows that in a limited area that a narrow current will produce a wider range of azimuths (Figure 16.1) and a wide current will produce a narrower range of azimuths (Figure 16.2).

Thus, Hereford's (1977) rose diagram and McKee's (1945) results correlate well with the concept of a pattern of large-scale depositional tongues (Figure 14) fanning out across Arizona to the east. Although a moving point source (storm or chattering point of slippage on a massive fault motion) for these currents may be simplistic, it does show the feasibility of a high-energy event causing the observed azimuth readings. If sedimentological analyses of bedforms and grains can support a corresponding flow velocity and depth, then this model will gain credibility. Thus, we need to evaluate the grain-size distribution found in the Tapeats Sandstone.

Grain-Size Distribution and Flow Characteristics

The grain-size distribution in strata does not represent the original depositional distribution. Finer grains, carried as suspended load, would occur as a fraction of their original abundance. McKee (1945, p. 51, brackets added) asserted: "skewness [in grain size] is due to competency rather than to lag material." In other words, grain sizes (the determining factor of competency) depend on the ratio of fines carried away

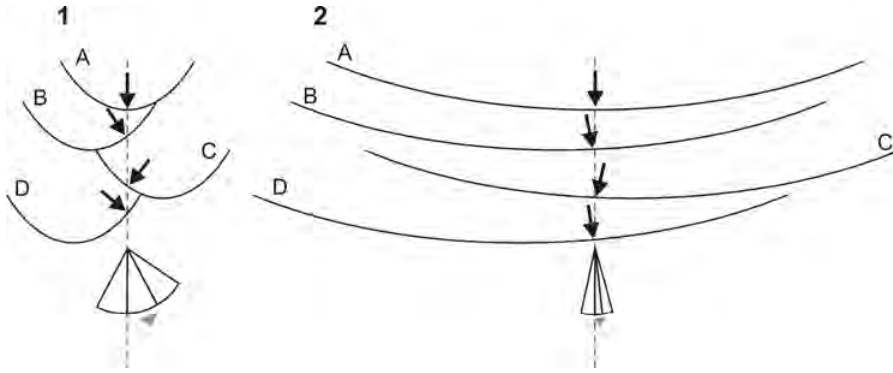


Figure 16. Aerial view of foreset azimuth readings taken through one vertical line through multiple narrow tongues of deposition (1) and wide depositional fronts with the same deviation after each flow (2). Arrows are perpendicular to front at the line and show direction of individual foresets. Sum of arrows shown as simplified rose diagram..

as suspended load to the sizes in the bed load. Careful examination of the grain-size distribution in sandstone can suggest the break in grain size between bed load that was deposited and suspended load that was not. This, in turn, can be used to estimate the flow velocity necessary to remove whatever size grains were carried as the suspended load.

Suspended load grains will not be totally absent because they settle at a constant rate called the *fall velocity*. The fall velocity of fine grains and their resultant rate of settling are largely independent of Bernoulli and turbulence forces (McLane, 1995) that keep larger particles moving above the laminar sublayer (Julien, 1998), where particle motion ceases and grains are deposited.

McKee (1945, his figure 4) took 24 samples of Tapeats Sandstone and measured their grain-size distribution. His histograms are converted to percent in Table I, and representative histograms are shown in Figure 17. Note that modern convention has fine to coarse sizes from left to right; thus, McKee's histograms are reversed. His histograms approximate a bell curve but are all skewed toward the coarser fraction. McLane (1995, his figure 2.2) showed a computer-simulated progression of grain sizes from a random sample of coarse

sediments (Figure 18). Between steps 4 and 6, the curve tails off, producing the characteristic lognormal curve. This skew to the finer fraction becomes more pronounced as the process continues. McLane (1995, p. 14, brackets added) asserted that "the function is not symmetrical but appears to lean towards the origin [positive skew], favoring the smaller values of the variate." Therefore, typical curves resulting from the random breakdown of coarser clasts are skewed to the finer grain sizes. However, this is exactly the opposite of the *observed* spread in all of McKee's histograms. They are all negatively skewed to the coarse fraction.

Despite McKee (1945, p. 39) having "taken [samples] from the upper half of the formation," they approximate a random sample because they are few in number and collected non-systematically over a large area. As such, they do reflect a relatively common distribution of grain sizes with the exception of samples *j* and *l*. These two are uniquely skewed further to the coarse end, perhaps as a result of being collected from a sandy debris flow (Barnhart, 2012a) or from the lag in a cut-and-fill structure. Since both *j* and *l* were collected from opposite sides of the same monadnock, and at the same distance from its peak, they may

both be from the same bedform. Additionally, sample *m* shows a calculation error in McKee's (1945) work, as it sums to a total of 116%. For these reasons, samples *j*, *l*, and *m* were excluded from the *mean* in Figure 17 and Table I. The remaining 21 samples are considered random and representative of normal grain sizes in the flow.

In discussing the separation of sediment between wash load (the part of sediment load moved primarily in suspension), mixed load, and bed load:

Einstein [1950] suggested that the largest size of washload may be arbitrarily chosen as the grain diameter, d_{10} , of which 10% by weight of the bed sediment is finer (Julien, 1998, p. 177, brackets added).

Although it is a valid generality, this might not hold true for a completely random collection of eroded sediment samples. For example, storm runoff may contain a higher percentage of coarse clasts, while farm soil may contain a higher percentage of clay and colloidal particles. However, this generalization should be valid for a well-sorted, mature sandstone like the Tapeats.

McKee's (1945) histograms (Table I and Figure 17) show a consistent break between very fine and fine sand and often a more pronounced break between fine and medium sand. Fine sand is never higher than 7% (Table I), and medium sand shows 10 of the 21 readings to be lower than 10%. Thereby using Einstein's (1950) method, the division between wash load and bed load is found in the range of fine and medium sand.

Another approach suggested by Julien (1998) separates wash load from bed load using the ratio (R_s) between shear (V_o) and fall (ω) velocities:

$$V_o / \omega = R_s \quad (1)$$

Julien (1998) gives a table for values of R_s based on the percent concentration of grain sizes carried in suspension (Table II). If percent is graphed versus

Table I. Grain-size percentages taken from histograms with location. From McKee (1945, his figure 4 and table 5).

| Grain Sizes (mm) | | | | | | | | | | |
|------------------|--------|--------|--------|--------|--------|-------|-------|---------|--------------------------------|----------------------------|
| Sample | < 0.06 | > 0.06 | > 0.12 | > 0.25 | > 0.50 | > 1.0 | > 2.0 | Total % | Geographic Location | Stratigraphic Location |
| <i>a</i> | 2 | 3 | 14 | 25 | 29 | 22 | 4 | 99 | Grand Wash | 50' below transition |
| <i>b</i> | 1 | 1 | 2 | 31 | 62 | 3 | 1 | 101 | Peach Springs Wash | upper transition |
| <i>c</i> | 2 | 4 | 6 | 38 | 41 | 8 | 2 | 101 | Peach Springs Wash | upper transition |
| <i>d</i> | 4 | 5 | 9 | 38 | 35 | 6 | 1 | 98 | Toroweep Valley | 10' below transition |
| <i>e</i> | 1 | 6 | 26 | 30 | 26 | 9 | 1 | 99 | Toroweep Valley | 20' below transition |
| <i>f</i> | 2 | 2 | 5 | 42 | 44 | 5 | 1 | 101 | 1/2 mile west of Kaibab Trail | 10' below top |
| <i>g</i> | 0 | 4 | 12 | 39 | 33 | 9 | 3 | 100 | West Fork Pipe Creek | 70' below top |
| <i>h</i> | 1 | 2 | 5 | 20 | 56 | 14 | 2 | 100 | West Fork Pipe Creek | 50' below top |
| <i>i</i> | 1 | 6 | 25 | 45 | 20 | 2 | 0 | 99 | East Fork Pipe Creek | 100' below top |
| <i>j</i> | 1 | 1 | 4 | 15 | 39 | 28 | 16 | 104 | SE of Yaki Point monadnock | 50' below top |
| <i>k</i> | 1 | 2 | 6 | 20 | 45 | 21 | 4 | 99 | NE of Yaki Point monadnock | 75' below top |
| <i>l</i> | 1 | 2 | 9 | 16 | 33 | 28 | 10 | 99 | NE of Yaki Point monadnock | 50' below top |
| <i>m</i> | 2 | 4 | 9 | 39 | 43 | 18 | 1 | 116 | Plateau Point | top |
| <i>n</i> | 2 | 4 | 19 | 35 | 28 | 11 | 1 | 100 | Plateau Point | 30' below top |
| <i>o</i> | 1 | 2 | 4 | 18 | 52 | 19 | 3 | 99 | Clear Creek Trail | 20' below top |
| <i>p</i> | 1 | 2 | 25 | 46 | 16 | 10 | 1 | 101 | Clear Creek Trail | 50' below top |
| <i>q</i> | 2 | 2 | 5 | 25 | 58 | 10 | 1 | 103 | Phantom Bay west end | lower cross-bedded |
| <i>r</i> | 2 | 5 | 9 | 27 | 53 | 5 | 0 | 101 | Phantom Bay west end | lower cross-bedded |
| <i>s</i> | 4 | 5 | 15 | 49 | 28 | 1 | 0 | 102 | Phantom Bay east end | flat bedded 30' above base |
| <i>t</i> | 4 | 7 | 12 | 48 | 28 | 1 | 0 | 100 | Phantom Bay east end | flat bedded middle |
| <i>u</i> | 1 | 1 | 4 | 18 | 65 | 10 | 1 | 100 | Phantom Bay east end | flat bedded top |
| <i>v</i> | 4 | 5 | 14 | 39 | 37 | 2 | 0 | 101 | Phantom Bay east end | flat bedded 2.5' below top |
| <i>w</i> | 1 | 3 | 16 | 36 | 39 | 5 | 1 | 101 | Phantom Bay east end | cross-bedded near base |
| <i>x</i> | 2 | 5 | 20 | 26 | 39 | 10 | 1 | 103 | Phantom Bay east end | cross-bedded base |
| <i>mean</i> | 1.86 | 3.62 | 12.05 | 33.10 | 39.71 | 8.71 | 1.33 | 100.38 | average without <i>j, l, m</i> | see text for explanation |

Table II. Modes of sediment transport given shear (V_0) and fall (ω) velocities. $V_0 / \omega = R_s$. $C_{0.8} = 0.75 C_{0.2}$ reads: the concentration at 80% of height from the bed equals 75% of the concentration at 20% of height from the bed. From Julien (1998, his table 10.2).

| R_s | Mode of Sediment Transport |
|---------|---|
| < 0.2 | No motion for all possible grain sizes |
| 0.2 | Lowest possible motion for turbulent flow over rough boundaries |
| 0.2–0.4 | Sediment transport as bed load |
| 0.4–2.5 | Sediment transport as mixed load |
| > 2.5 | Sediment transport in suspension |
| 25 | $C_{0.8} = 0.75 C_{0.2}$ |
| 100 | $C_{0.8} = 0.93 C_{0.2}$ |
| 400 | $C_{0.8} = 0.98 C_{0.2}$ |

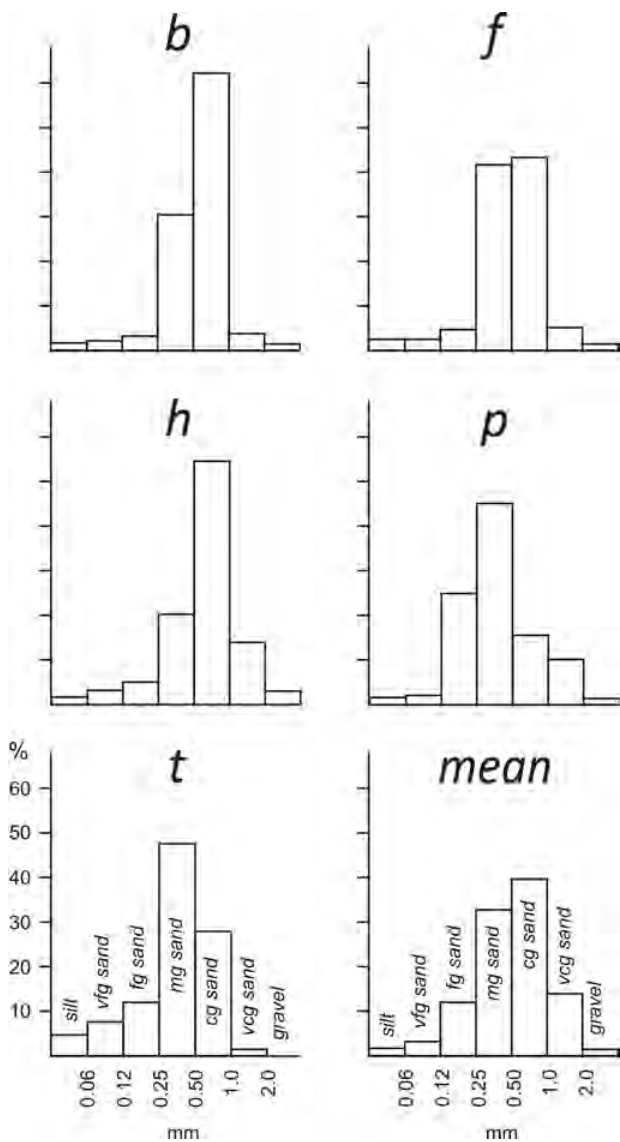


Figure 17. Histograms of grain-size distribution. Five samples taken from McKee (1945, his figure 4) and the calculated mean. See text for discussion.

the R_s values, Figure 19 can be used to extrapolate the suspended load as a percent of the total load. Values for at 20° C, obtained from Julien (1998), and R_s values from Table II, rearranging formula (1), V_0 is derived and compared in Table III. Using Figure 19, these values convert to the percentage of grains missing in each size range up to and including the suspended load.

Converting McLane’s (1995) graph in Figure 18 step 8 to a line, McKee’s (1945) histogram h and the mean derived in this study (Figure 17) are imposed below the lognormal line (Figure 20.1 and 20.2). The lognormal distribution curve from McLane and McKee’s histograms do not appear similar in shape, especially in the first 5 grain-size columns (up to coarse sand). This illustrates the positive and negative skew discussed above. If the first columns are underrepresented, it is likely due to the loss of suspended load in transport. Table III gives the percent suspended by grain size at various shear velocities.

In Figure 20.4, McKee’s mean histogram and lognormal curve, comparing the point of suspension, at $V_0 = 15$ cm/s (0.15 m/s) the coarse sand fraction is still less than 10% in suspension and is thus the closest critical grain size (Einstein, 1950). At the same shear velocity, the very fine sand has reached 82% in suspension. This means that the fraction shown on the mean histogram measuring 3.62% of the total grains would represent less than one percent considering the original grain concentration for that size range.

Comparing the lognormal line of McLane’s and McKee’s histogram h in Figure 20.3, the change seems to be in the area of $d > 1.0$ mm, very coarse sand. At 30 cm/s (0.3 m/s) from Table III, the fraction $d > 1.0$ mm passes the critical 10% portion in suspension, and so that column and all those to the left would be overrepresented in McKee’s (1945) histogram. For the $d > 0.0625$ mm, the very fine sand fraction at 30 cm/s, Table III shows 92% suspended load. Table I

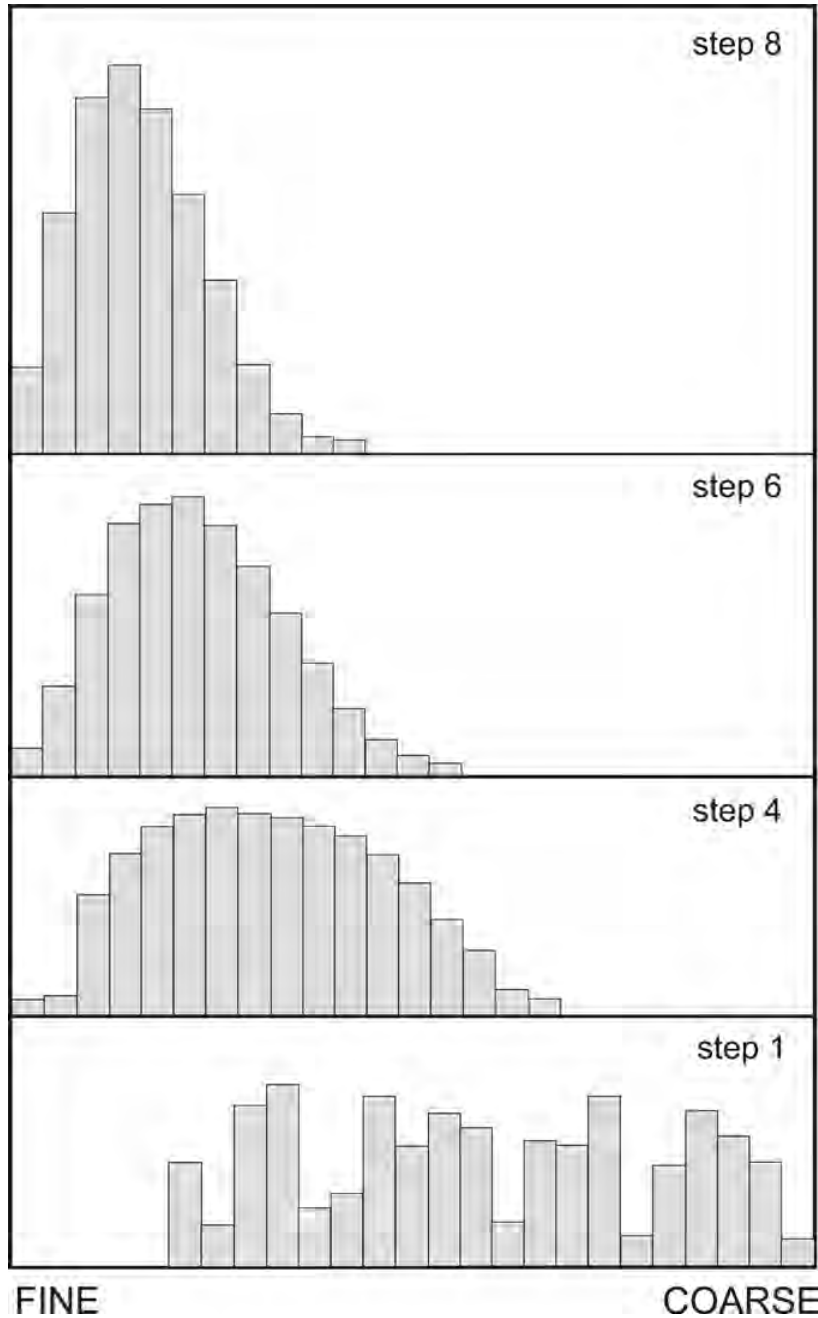


Figure 18. Histogram of computer-simulated progression from random clast size to lognormal distribution of smaller sizes after repeated application of proportional-effect rule. From McLane (1995, his figure 2-2 showing his steps 1, 4, 6, and 8).

shows $d > 0.06 = 2\%$ of the total, and if the total under the lognormal curve for $d > 0.06$ is approximately 20% then the adjusted amount for very fine sand would be about 2%. Similar adjustments must be made for each column

in Figures 20.3 and 20.4. The hatched area would be the grains missing, based on the calculations in Table III using the R_s method. Figure 20.4, the mean, would represent deposition under shear velocity (V_0) of 0.3 m/s.

Shear velocity is the flow velocity at the boundary layer, where a stable particle is put into motion. It is almost always much slower than the average velocity higher in the flow. Ruben and McCulloch (1980), using Keulegan's (1938) classic work, give the following formula for converting between the two velocities, where h = flow depth and f = friction factor:

$$=V_0 (5.75 \log (0.37 h/f)) \quad (2)$$

Lalomov (2007, p. 276) provided the formula for Keulegan's friction factor (f), where d = critical grain diameter:

$$f = (2.03 \log (12.2 h/d_{max}))^2 \quad (3)$$

Table IV shows representative conversions between shear and average velocity for possible flow depths.

For Figure 20.4 and $V_0 = 0.15$ m/s, using $d > 0.5$ mm as the critical grain size for determining suspension and assuming the shallowest depth of flow that would deposit a 10 cm (3.93 in)-thick compound cross bed, Table IV yields an average flow velocity of 1.04 m/s. As flow depth increases (for thicker layers), up to $h = 9.0$ m, increases to 2.24 m/s. Using Figure 20.3 and using $V_0 = 0.3$ m/s, $d > 1.0$ mm as the critical grain size, and a minimal depth of 0.6 m, we find that = 1.96 m/s. For the greater depth of 9.0 m, = 4.38 m/s.

A possible environmental explanation for these numbers would be a wave. It would begin by depositing the thicker diagonal flat beds (compound cross bedding) at the maximum depth of 9 m (30 ft) and a velocity of over 4 m/s (about 9 mph). As the wave passed, it would deposit the thinner horizontal flat beds as the depth decreased to less than a meter and the tail velocity of the wave diminished to about 2 m/s (about 4.5 mph).

These velocities will result in the deposition of dunes to upper-regime flat beds (Figures 21.1 and 21.2). As

Table III. Shear velocities and R_s factors for histogram separation of sizes when deposited at various velocities. Percentages represent % solids as read from Figure 19.

| column | d (mm) | W (cm/s) | $V_o = 10$ cm/s | | $V_o = 15$ cm/s | | $V_o = 20$ cm/s | | $V_o = 30$ cm/s | | $V_o = 40$ cm/s | |
|--------|-----------------------|----------|-----------------|------|-----------------|------|-----------------|------|-----------------|-----|-----------------|-----|
| | | | R_s | % | R_s | % | R_s | % | R_s | % | R_s | % |
| 1 | < 0.0625 SILT | --- | --- | --- | --- | --- | --- | --- | --- | --- | --- | --- |
| 2 | > 0.0625 VERY FINE | 0.347 | 29 | 77 | 43 | 82 | 58 | 86 | 86 | 92 | 115 | 94 |
| 3 | > 0.125 FINE | 1.28 | 7.8 | 52 | 11.7 | 59 | 15.6 | 68 | 23 | 72 | 31 | 78 |
| 4 | > 0.25 MEDIUM | 3.6 | 2.8 | 20 | 4.2 | 34 | 5.6 | 43 | 8.3 | 53 | 11 | 58 |
| 5 | > 0.5 COARSE | 7.03 | 1.42 | < 10 | 2.1 | < 10 | 2.8 | 20 | 4.3 | 34 | 5.7 | 41 |
| 6 | > 1.0 VERY COARSE | 11.2 | --- | --- | --- | --- | 1.8 | < 10 | 2.6 | 15 | 3.6 | 28 |
| 7 | > 2.0 GRAVEL | --- | --- | --- | --- | --- | --- | --- | --- | --- | --- | --- |

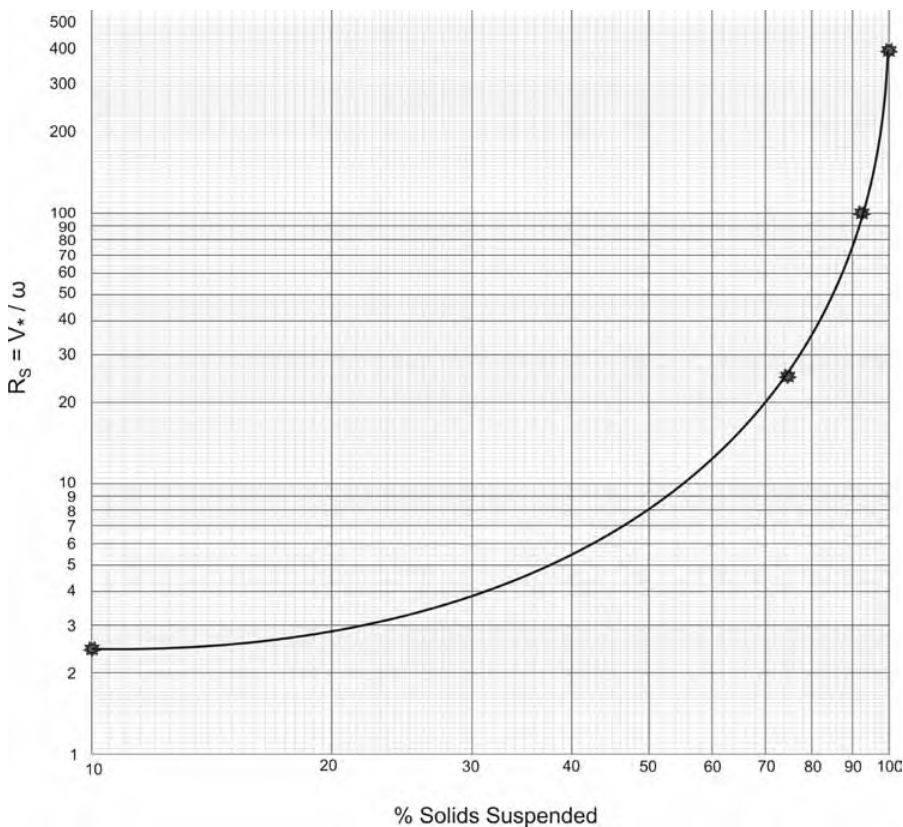


Figure 19. Percent of clasts carried in suspension as determined by R_s values. Graphed curve based on four points of Julien (1998, p. 188) marked with stars. See also Table III.

noted above, changes between these two bedforms are a function of competency, which in turn varies with depth; changes in rheology are not necessary. As both are high-velocity bedforms, the current was most likely a high-velocity unidirectional current.

What became of the missing fine fraction represented by the hatch marks in Figure 20.3 and 20.4? Hereford (1977) did not provide significant grain-size information for central Arizona; thus it is unclear whether or not grain size decreases downstream. Or are fines simply missing because they were transported out of the area? This question needs further research.

Rhythmic Patterns and Rate of Deposition

Figure 22 is an outcrop in the eastern part of Chuar Canyon (Figure 1), where the still-plastic sandstone of the Tapeats is deformed and tilted upward. The East Kaibab monocline runs north-south for about 300 km (186 miles) and probably extends both north and south beyond its exposure (Huntoon, 2003). Although this post-depositional deformation absent extensive fracturing is an interesting

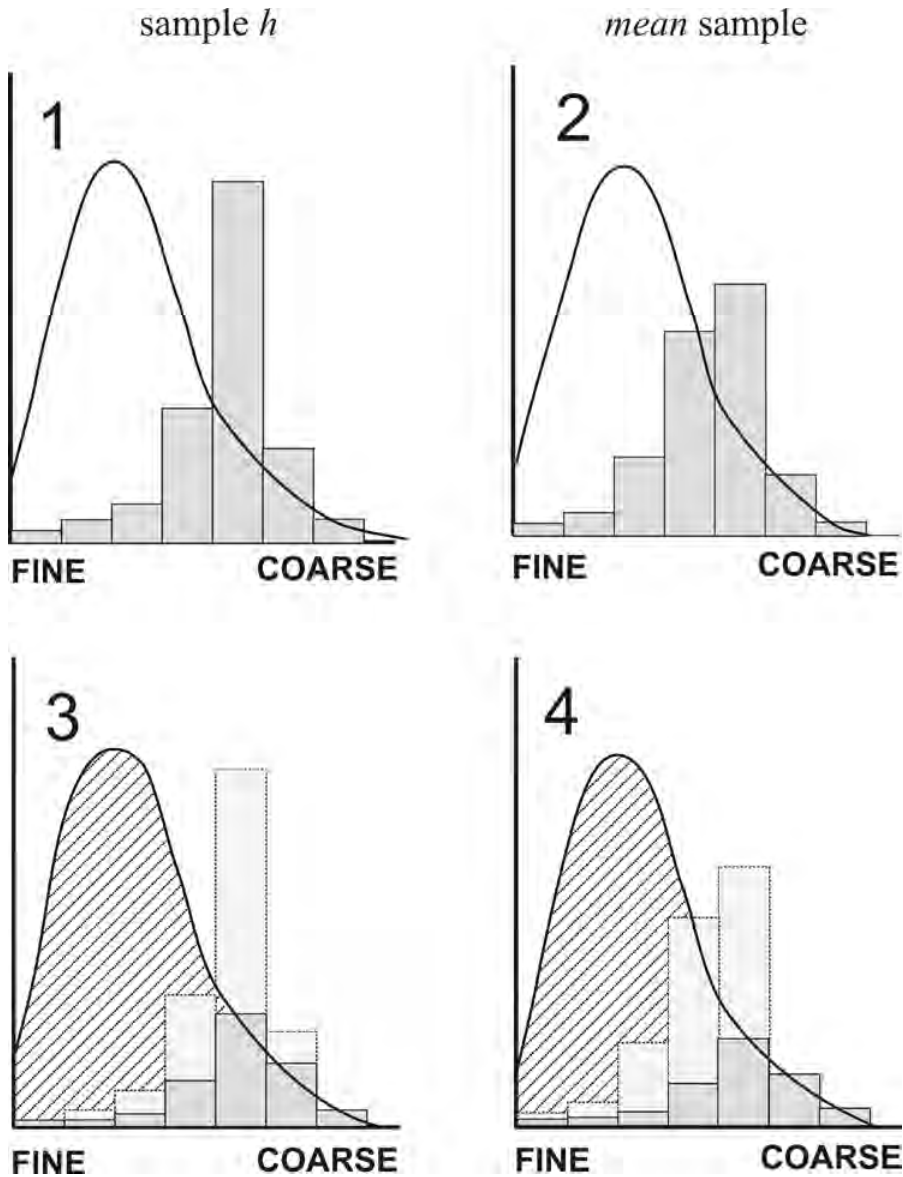


Figure 20. Comparison of lognormal curve from Figure 18, step 8, superimposed over (20.1) a representative sample (p) from McKee (1945, his figure 4), and (20.2) *mean* from Figure 17. 20.3 and 20.4 are same samples with histograms adjusted to reflect percentages of original lognormal grain sizes still present. Hatched areas represent missing clast due to suspension in wash load.

question (cf., Snelling, 2009), this study is more interested in the alternating thick and thin layers in the Tapeats at this location. Figure 22 shows nine of these repetitions at about 3 m thick, while Figure 4 shows greater detail of five repetitions.

Similar repetitions were observed in the Hurricane Katrina splay deposits (Barnhart, 2011), interpreted as evidence of repeated pulses of energy. Those alternating beds repeated at intervals of 18–25 cm (7–9.8 in) and were interpreted as products of the rhythmic

passing of storm surges as the waves propagated down the canal from Lake Pontchartrain and through the breach, each leaving deposits about 3 cm (1.18 in) thick.

In Figure 4 a similar pattern can be seen in a 1.0–1.5 m (3.3–4.9 ft)-thick group of thin layers, each about 3–4 cm (1.18–1.57 in) thick, separated by a thick layer of cross bedding about 1.5 m thick, or by several thinner layers about 10 cm (3.93 in) thick. The complete cycle makes a repeating pattern about 2.5–3.0 m (8.2–9.8 ft) thick, which is consistent with the approximate 3.0 m rhythmic pattern of Figure 22.

Allen (1976) estimated flow depth to be about 6–8 times dune height, which suggests flow depth of 0.3–12 m (0.98–39.4 ft). Based on modern storms, the initial wave at the front of the storm surge would be larger, followed by less energetic waves between storm pulses. While there is no firm evidence in the Tapeats for a causal mechanism, a repeating sequence of relatively small waves interspersed by larger waves (up to 12 m) would be consistent with large compressional waves produced at regular intervals by a storm or by significant recurring fault motions but cannot be explained by normal tidal cycle deposition, as proposed by secular geologists. The Tapeats does not conform to modern facies models.

Another failure of modern facies models is found in the energy at deposition. Barnhart (2012a) estimates it at 9–54 m/hr (29.5–177 ft/hr) for the lower Tapeats. Given the thickest measured section of Tapeats (Noble, 1922, at the Bass Trail) is 120 m (393 ft), the entire sequence could have been deposited in as little as 3 hours. No modern depositional environment provides an analog for that scale and rate of sedimentation. Though the rate seems very high, the wave pattern—one 12 m wave followed by smaller waves repeating at a rate of the largest wave every 10 minutes—yields a total depositional rate of 15–18

Table IV. Some shear velocities converted to average velocities for some representative flow depths. Froude numbers (Fr) provide a relative measure of flow agitation as it approaches $Fr = 0.84$ where antidunes start to form.

| d (m) | h (m) | f | $V_o = 0.1$ | Fr | $V_o = 0.15$ | Fr | $V_o = 0.2$ | Fr | $V_o = 0.3$ | Fr | $V_o = 0.4$ | Fr |
|---------|---------|-------|-------------|------|--------------|------|-------------|------|-------------|------|-------------|------|
| 0.001 | 0.6 | 0.016 | 0.65 | 0.27 | 0.98 | 0.40 | 1.31 | 0.54 | 1.96 | 0.81 | 2.61 | 1.07 |
| 0.0005 | 0.6 | 0.014 | 0.69 | 0.28 | 1.04 | 0.42 | 1.38 | 0.57 | 2.07 | 0.85 | 2.76 | 1.14 |
| 0.00025 | 0.6 | 0.012 | 0.73 | 0.30 | 1.09 | 0.45 | 1.45 | 0.58 | 2.18 | 0.93 | 2.90 | 1.19 |
| 0.001 | 3.0 | 0.012 | 1.14 | 0.21 | 1.71 | 0.32 | 2.28 | 0.42 | 3.41 | 0.63 | 4.56 | 0.84 |
| 0.0005 | 3.0 | 0.010 | 1.17 | 0.22 | 1.75 | 0.32 | 2.34 | 0.43 | 3.51 | 0.65 | 4.68 | 0.86 |
| 0.00025 | 3.0 | 0.009 | 1.20 | 0.22 | 1.80 | 0.33 | 2.40 | 0.44 | 3.60 | 0.66 | 4.80 | 0.89 |
| 0.001 | 6.0 | 0.010 | 1.34 | 0.17 | 2.01 | 0.26 | 2.68 | 0.35 | 4.03 | 0.53 | 5.36 | 0.70 |
| 0.0005 | 6.0 | 0.009 | 1.37 | 0.17 | 2.06 | 0.27 | 2.74 | 0.36 | 4.12 | 0.54 | 5.48 | 0.71 |
| 0.00025 | 6.0 | 0.008 | 1.40 | 0.18 | 2.10 | 0.27 | 2.80 | 0.37 | 4.20 | 0.55 | 5.60 | 0.73 |
| 0.001 | 9.0 | 0.010 | 1.46 | 0.16 | 2.19 | 0.23 | 2.92 | 0.31 | 4.38 | 0.47 | 5.84 | 0.62 |
| 0.0005 | 9.0 | 0.009 | 1.49 | 0.16 | 2.24 | 0.24 | 2.98 | 0.32 | 4.47 | 0.48 | 5.96 | 0.63 |
| 0.00025 | 9.0 | 0.008 | 1.52 | 0.16 | 2.28 | 0.24 | 3.04 | 0.32 | 4.56 | 0.49 | 6.08 | 0.65 |

m/hr (49–59 ft/hr). Even the lower end would deposit the entire Tapeats 120 m thickness in only 8 hours. At that same rate, the entire thickness of the Grand Canyon sedimentary sequence (1,829 m, or 6,000 ft) would require only 122 hours. Of course, this does not include thickness lost to erosion or compaction, but the essential point remains: the Tapeats was laid down in hours, not millions of years.

Even creationists can underestimate the depositional potential of the Flood. At these rates, much of the sedimentary record could have been deposited even in the first 40 days of the Flood! As Henry Morris (2003, p. 7) wisely said:

Veneration of the Bible for its 'spiritual value' only is ... inconsistent with rejection of its scientific and historical teachings. If the latter cannot be trusted—that is, statements which

are susceptible to actual human investigation and proof—then how can its spiritual teachings, which are not susceptible of proof, be trusted?

Conclusion

Classic studies of the Tapeats Sandstone have interpreted its depositional environment as a low-energy beach or nearshore settings, promoting slow deposition and a facies model approach. However, the different approach of these two papers has shown that template to be inadequate; the hydrodynamic method suggests a quite different mode of deposition.

Monadnocks are not the scattered remnants of shoreline highlands, but are infrequent irregularities in a rapidly formed planation surface in excess of 23,000 km² (8,880 miles²) cut into both

crystalline basement and sedimentary strata (Figure 23B). They are typically a few meters high, though some reach as high as 140 m, and the only breccia that remains is in scattered aprons in close proximity to some of the highs. These scattered elevations resulted from the vagaries of the current and are independent of the substrate hardness. Immediately following erosion, while breccia remained on the monadnocks (Figure 23C), the inrushing high-velocity hyperconcentrated current (Figure 23D), probably accompanied by considerable precipitation, washed the loose breccia down into the incoming current (Figure 23E), producing high-density turbulent currents that deposited cross beds from sandy debris flows (Figure 23F) within the otherwise flat hyperconcentrated laminae (Figure 23G) formed by the primary current.

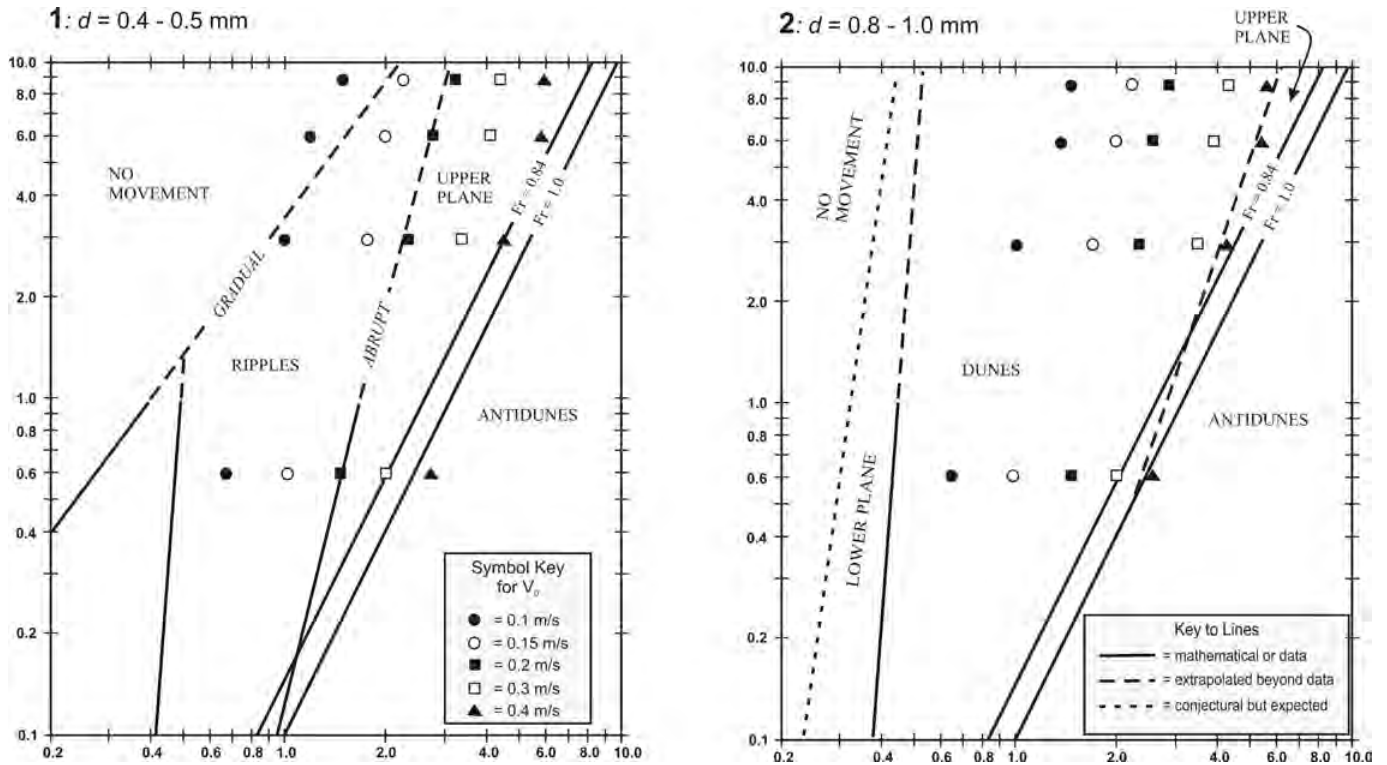


Figure 21. Bedform stability graphs for grain sizes (21.1) $d = 0.4-0.5$ mm and (21.2) $d = 0.8-1.0$ mm. Solid lines represent transitions between bedforms as presented by Southard and Buguchwal (1990, their figures 2H and 2K) and mathematical derivation. Dotted lines extrapolated beyond data. Long dashed line conjectural but expected. Symbols show values of shear velocity (V_0) at varied flow depths as represented in Table IV.

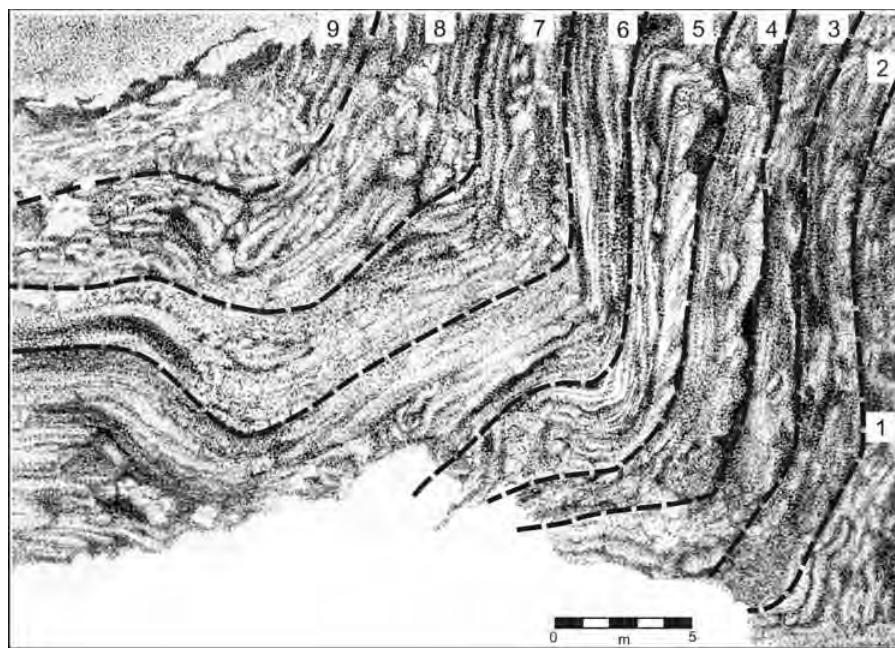


Figure 22. Chuar Canyon (Carbon Canyon?) exposure of East Kaibab monocline showing nine repetitions of thick and thin sequences. Modified from Snelling (2009).

The depositing current, with 20–30% solids, was plastic, like a mudflow off a steep, denuded hillside after a heavy rain. However, the Tapeats was deposited across a broad flat plain with a slope of only about 0.001 or 0.14%, and with no nearby highlands to provide the gradient and thus the energy for the current. That the monadnocks are not a residual highland at the time of deposition is seen in their only minor effect on the broad laminar bedforms; the sandy debris flows caused by cascading breccia are quite limited in extent.

This high-velocity hyperconcentrated current flowed northeast to southwest and was shallow—1–2 m—but reached velocities of 2.0–4.7 m/s (4.5–8 mph). In comparison, the present-day Colorado River flows at around 3 mph. With no nearby gradient, it is likely that this current, as broad as it was, was instead powered by the head pres-

sure of a large storm surge or by that created by crustal motion. It was also abrupt; whatever water was present beforehand (but after planation) was insufficient to transport the breccia off the monadnocks.

The nature of the current is seen in the Tapeats sands; deposition was so rapid

that the sequence of the lithology was dependent on the order of entrainment and the sorting provided by the highly turbulent flow. There is little evidence of post-depositional reworking or differential settling. At no time did this high-velocity, unidirectional current provide any period of slack energy within its flow.

As sedimentation progressed to the middle and upper Tapeats, more water was entrained with the sediments and the rheology changed from plastic to fluidal flow. With deposition taking place across a 300-km front, the current separated into multiple shifting tongues (Figure 23H). Increasing fluidal conditions resulted in decreased viscosity and increased velocity to over 4 m/s (9 mph). Individual tongues were still highly turbulent under their 12 m wave fronts (Figure 23I). Higher energy at the wave front eroded channels into the unconsolidated substrate (Figure 23J), resulting in cross beds up to 1.5 m followed by thin high-velocity flat beds deposited in the shallowing wave train (Figure 23K), which had increased competency. These sets of strata reached 3 m; each deposited by a major wave front and the following wave train. This rhythmic repetition of bedforms persists for over 200 km along the axis of flow. This pattern

Table V. Revised velocities calculations based on lower slopes and increased flow depth (*h*). Set of velocities obtained by increasing Froude number to 1.2.

| <i>S</i> | <i>d</i> _{max} (m) | % solid (vol) | <i>τ</i> ₀ (Pa) | <i>h</i> (m) | <i>n</i> | \bar{V} (m/s) | Fr | \bar{V} (m/s) at Fr = 1.2 |
|----------|-----------------------------|---------------|----------------------------|--------------|----------|-----------------|------|-----------------------------|
| 0.0014 | 0.038 | 20 | 24.6 | 1.35 | 0.0156 | 2.85 | 0.78 | 4.37 |
| | | | 21.6 | 1.05 | | 2.44 | 0.76 | 3.85 |
| | 0.064 | 30 | 41.5 | 2.28 | | 4.10 | 0.87 | 5.67 |
| | | | 36.3 | 1.77 | | 3.46 | 0.83 | 5.00 |

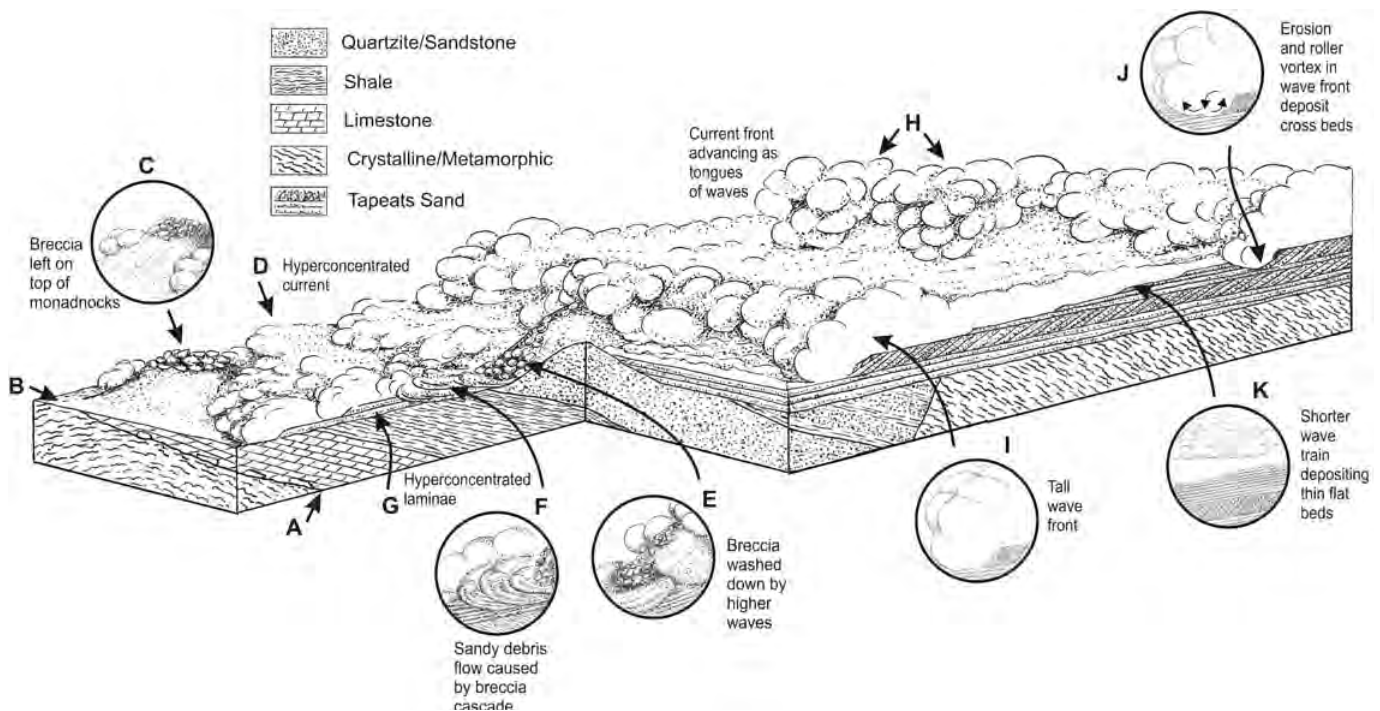


Figure 23. Cartoon diagram of lithology in the Tapeats and its spatial relationship to lithology below the (A) Greater Unconformity and (B) Great Unconformity planation surface. Comparative height and turbulence of waves from the northeast to southwest is suggested. See text for further explanation.

of waves is reminiscent of storm waves created by hurricanes or compressional waves generated by stuttering crustal motions such as submarine earthquakes.

The high velocity of the initial wave in the train is suggested by the tangential toe contact of the cross bedding and in the internal compound cross bedding. The presence of tangential toe contacts in the cross beds associated with the high-velocity flat beds shows no significant loss of velocity, only a change in competency, with a decrease in depth to only 0.3 m. If a wave train passed a given point every 10 minutes, a depositional rate of only 1.5 m per wave train would deposit the entire 120 m thickness of the Tapeats in only 8 hours. If a wave train striatal package was 3 meters per wave, the Tapeats would have been deposited in as little as 4 hours.

There is no clear evidence as to whether or not deposition took place under subaerial conditions with significant precipitation or as a hyperpycnal flow under standing water. Perhaps it was the former since precipitation would add extra water to produce fluidal flow. However, it is hard to imagine the necessary waves moving over such broad distances with such shallow water on almost no gradient. Further research may offer better explanations as it shows subtle changes in the bedforms over the full flow distance.

An interesting inference of this hydrodynamic assessment is the surprising presence of trace fossils in such a high-energy environment. *Diplocraterium* occur in the tangential toe contacts of cross bedding and throughout the upper Tapeats. Typical interpretations would suggest a low-energy, stable marine environment. This strongly suggests that these traces are escape structures generated by organisms transported inland by the wave trains. It implies that the presence of ichnofossils should not immediately preclude deposition under high-energy conditions.

Acknowledgments

I appreciate the help and encouragement of several friends, especially Sandia. I also appreciate the work of Berthault, Lalomov, and Julien, that has shown the value of this approach. Most of all, I thank God for giving me ideas and persistence to follow through.

References

- Allen, J.R.L. 1976. Bedforms and unsteady processes: some concept of classification and response illustrated by common one-way types. *Earth Surface Processes* 1:361–374.
- Barnhart, W.R. 2011. Hurricane Katrina splay deposits: hydrodynamic constraints on hyperconcentrated sedimentation and implications for the rock record. *Creation Research Society Quarterly* 48:123–146.
- Barnhart, W.R. 2012a. A Hydrodynamic interpretation of the Tapeats Sandstone, Part I: basal Tapeats. *Creation Research Society Quarterly* 48:288–311.
- Barnhart, W.R. 2012b. Transgression/regression in the Grand Canyon. *Creation Research Society Quarterly* 48:352–354.
- Barwis, J.H., and M.O. Hayes. 1985. Antidunes on modern and ancient washover fans. *Journal of Sedimentary Petrology* 40(4):1095–1127.
- Berthault, G. 2002. Analysis of the main principles of stratigraphy on the basis of experimental data. *Lithology and Mineral Resources* 37(5):442–446.
- Cowart, J.H., and C.R. Froede Jr. 1994. The use of trace fossils in refining depositional environments and their application to the creationist model. *Creation Research Society Quarterly* 31:117–124.
- Einstein, H.A. 1950. The bed load function for sediment transport in open channel flows. *Technical Bulletin No. 1026*. U.S. Department of Agriculture, Soil Conservation Service, Washington, DC.
- Froede, C.R., Jr. 2009. Sediment bioturbation experiments and the actual rock record. *Journal of Creation* 23(3):3–5.
- Hereford, R. 1977. Deposition of the Tapeats Sandstone (Cambrian) in central Arizona. *Geological Society of America Bulletin* 88:199–211.
- Huntoon, P.W. 2003. Post Precambrian tectonism in the Grand Canyon region. In Beuss, S.S. and M. Morales (editors). *Grand Canyon Geology*, second edition, pp. 222–259. Oxford University Press, New York, NY.
- Julien, P. 1998. *Erosion and Sedimentation*. Cambridge University Press. New York, NY.
- Julien, P., Y. Lan, and G. Berthault. 1994. Experiments on stratification of heterogeneous sand mixtures. *TJ* 8(1):37–50.
- Keulegan, G.H. 1938. Laws of turbulent flow in open channels. *U.S. National Bureau of Standards Research Journal* 21:707–741.
- Klein, G. deV. 1970. Depositional and dispersal dynamics of intertidal sand bars. *Journal of Sedimentary Petrology* 40(4):1095–1127.
- Ladd, G. 2007. Photo inside front cover. *Arizona Highways* 83(6).
- Lalomov, A.V. 2007. Reconstruction of paleohydrodynamic conditions during the formation of Upper Jurassic conglomerates of the Crimean Peninsula. *Lithology and Mineral Resources* 42(3):268–280.
- Mason, T.R., and A.D.M. Christie. 1986. Paleoenvironmental significance of ichnogenus *Diplocraterion Torell* from the Permian Vryheid Formation of the Karoo Supergroup, South Africa. *Paleogeography, Paleoclimatology, Paleoecology* 52(3–4):249–265.
- McKee, E.D. 1945. Stratigraphy and ecology of the Grand Canyon Cambrian, part I. In *Cambrian History of the Grand Canyon Region*. Carnegie Institute of Washington Publication 563.
- McKee, E.D., E.J. Crosby, and H.L. Berryhill, Jr. 1967. Flood deposits, Bijou Creek, Colorado, 1965. *Journal of Sedimentary Petrology* 37:829–851.
- McLane, M. 1995. *Sedimentology*. Oxford University Press, New York, NY.
- Middleton, L.T., and D.K. Elliot. 2003. Tonto Group. In Beuss, S.S., and M. Morales (editors). *Grand Canyon Geol-*

- ogy, second edition, pp. 90–106. Oxford University Press, New York, NY.
- Morris, H.M. 2003. *Biblical Catastrophism and Geology*. Institute for Creation Research, Santee, CA.
- Nelson, S.A., and S.F. LeClair. 2006. Katrina's unique splay deposits in a New Orleans neighborhood. *Geological Society of America Today* 16(9):4–10.
- Neuendorf, K.K.E., J.P. Mehl Jr., and J.A. Jackson. 2005. *Glossary of Geology*, 5th Edition. American Geological Institute, Alexandria, VA.
- Nichols, G. 1999. *Sedimentology and Stratigraphy*. Blackwell Publishing, Boston, MA.
- Noble, L.F. 1922. A section of the Paleozoic formation of the Grand Canyon at the Bass Trail. *USGS Professional Paper* 131-B:23–73 (cited in Middleton and Elliot, 2003, p. 93).
- Oard, M.J. 2011. The remarkable African Planation Surface. *Journal of Creation* 25(1):111–122.
- Rose, E.C. 2006. Nonmarine aspects of the Cambrian Tonto Group of the Grand Canyon, USA, and broader implications. *Paleoworld* 15:223–241.
- Rubin, D.M., and D.S. McCulloch. 1980. Single and superimposed bedforms: a synthesis of San Francisco Bay and flume observations. *Sedimentary Geology* 26:207–231.
- Schumm, S.A., and H.R. Khan. 1972. Experimental study of channel pattern. *GSA Bulletin* 83:1755–1770.
- Smith, N.D. 1972. Some sedimentological aspects of planar cross-stratification in a sandy braided river. *Journal of Sedimentary Petrology* 42(3):624–634.
- Snelling, A.A. 2009. Rock layers folded, not fractured: Flood evidence number six. *Answers* 4(2). <http://www.answersingenesis.org/articles/an/v.4/n.2/folded-not-fractures>. (May, 2010).
- Sohn, Y.K., M.Y. Choe, and H.R. Jo. 2002. Transition from debris flow to hyperconcentrated flow in a submarine channel (the Cretaceous Cerro Toro Formation, southern Chile). *Terra Nova* 14:405–415.
- Southard, J.B., and L.A. Boguchwal. 1990. Bed configuration in steady unidirectional water flows; part 2, synthesis of flume data. *Journal of Sedimentary Research* 60:658–679.